A model set-up for an oxygen and nutrient flux model for Aarhus Bay (Denmark)

[Blank page]

A model set-up for an oxygen and nutrient flux model for Aarhus Bay (Denmark)

Henrik Fossing
National Environmental Research Institute

Peter Berg
University of Virginia

Bo Thamdrup
University of Southern Denmark

Søren Rysgaard
National Environmental Research Institute

Helene Munk Sørensen
County of Aarhus

Kurt Nielsen
National Environmental Research Institute

Data sheet

Abstract:	Most of the organic matter found in the sea is degraded in the seabed. A number of different bacteria are responsible for organic matter degradation. Through their metabolic processes bacteria form inorganic nitrogen and phosphorus compounds that are thus made available for new production. They also produce a number of waste products, such as hydrogen sulphide, that have a great impact on the marine environment. After many years of research, our knowledge of the processes going on in the seabed is substantial. This knowledge forms the basis of a new mathematical model linking the complex material cycles taking place in the seabed and describing the exchange of oxygen and nutrients between seabed and seawater. The construction of the model is described in this report. This report was prepared as a contribution towards developing NERI's expertise within the field of mathematical modelling.

Contents

National Environmental Research Institute

Technical reports from NERI

[Blank page]

Introduction

The subject of this report is the construction and application of a mathematical model describing the degradation of organic material in the seabed and the exchange of nutrients and oxygen between the seabed and the water column. The model was set up for Aarhus Bugt, Denmark and is based on a model concept developed for Young Sound, Northeast Greenland. Compared with the Northeast Greenland model the model described here has been developed further and adapted to temperate estuarine systems, and phosphorus cycling has been integrated into the model.

Since the mid-20th century nutrient cycling in the seabed has been studied in many locations worldwide and is described in detail in the scientific literature. Thus, today our knowledge of the many degradation processes in the seabed and the coupling between them is extremely good. In fact, so much knowledge is now available in this field that we believe it possible to set up a mathematical model describing: 1) processes involved in degradation of organic material in the seabed, 2) the release of the nutrients nitrogen and phosphorus from the seabed and 3) the nutrient balance between sediment and bottom water, which is the key factor determining whether nitrogen and phosphorus are taken up in the sediment or released to the water column.

The model is constructed so as to react to the amount of organic material reaching the seabed, to temperature and to bottom-water concentrations of oxygen, nitrogen and phosphorus. If the organic load to the seabed or the bottom-water nitrogen concentration is changed, for instance, the model can be used to predict how the seabed will react to these environmental changes. One might wish to be able to predict future changes in nutrient release from or take-up in the seabed, or the time that will elapse before these changes make themselves felt. Therefore, this type of model is a highly applicable tool for setting up scenarios of the response of sediment conditions and nutrient release to changes in the environmental status of estuaries and concomitant changes in organic load to the seabed.

In the field of biogeochemical research – that is, research into biological and (geo)chemical processes in the seabed – the oxygen and nutrient flux model, which, in this context, one might also refer to as a biogeochemical or diagenetic model, may be very useful. When the model was under construction, it soon became necessary to take into account sediment processes that had been verified through laboratory studies but had not been shown to take place in situ. In this way, the model can also be used to render probable the existence of biogeochemical sediment processes, which we do not possess the techniques to prove or measure in situ, but which must take place, nonetheless, if we are to explain the concentration changes that we observe from year to year. In other words, even though we cannot measure many of the biogeochemical processes in the sediment, the

model enables us to not only render the processes probable but to calculate process rates as well.

First, we set up the mathematical model, which we also refer to as the oxygen and nutrient flux model, or just "the model", on the basis of our knowledge of degradation processes in the sediment and of the coupling between the different nutrient cycles. We then modified the model by use of a comprehensive dataset from Aarhus Bay obtained under The Marine Research Programme 1990 (HAV90) (implemented in connection with the passage of the Danish Action Plan for the Aquatic Environment in 1987).

The studies in Aarhus Bay were carried out during more than 1½ years in the early 1990s through close collaboration between researchers from Danish universities, sector research institutions and the County of Aarhus, and covered a variety of investigations ranging from the production of organic matter in the water column to organic matter degradation in the sediment. The purpose of these studies was to examine how organic matter reaching the seabed was degraded and in which way the degradation processes influenced the nitrogen and phosphorus balance between seawater and sediment.

Collection of seawater and sediment samples was arranged in such a way that organic matter degradation and nitrogen and phosphorus exchange could be measured directly to the greatest possible extent. Furthermore, it was important to the research project that sampling should take place over a long period of time and with sufficient frequency to ensure that the results of our efforts provided the best possible description of the annual cycle in Aarhus Bay. Thus, water and sediment samples were collected at 2-3-week intervals in the period 1 January 1990- 31 May 1991. This approach ensured sufficient seasonal overlap to make the observations from Aarhus Bay – made more than 10 years ago – the most comprehensive dataset to date describing the annual cycle in a coastal marine ecosystem.

The results of the many studies are described in the publication series: *Marine research from the Danish Environmental Protection Agency.* Besides the many reports in Danish, research results have been published in a large number of international journals. If you would like to learn more about the studies, please see the publication list at the back of this report.

This report is arranged in the following way:

In *Chapter 1* we go through the degradation of organic matter with focus on the processes taking place in the seabed. We present the chemical reactions that make up the model and describe how the many reactions interact to form what we call the nutrient cycles. Chapter 1 presents the theoretical and practical knowledge that forms the basis of the mathematical model describing the degradation of organic matter in the seabed.

In *Chapter 2* we set up the oxygen and nutrient flux model for Aarhus Bay and the construction and calibration of the model are

described in detail. Model calculations of concentration profiles in the sediment and the exchange of nutrients and oxygen between sediment and water column are compared with results from the extensive investigations in Aarhus Bay in 1990-91.

1 Nutrient cycling in the seabed

The production of organic matter by plants, primary production, forms the basis of life in the ocean. Through photosynthesis, plants assimilate carbon dioxide (CO_2) and produce oxygen (O_2), while at the same time taking up inorganic nutrients and incorporating them into organic compounds. The organic matter passes through the food web, and a large portion of primary production sooner or later ends up on the seabed. Even as dead organic matter is sinking through the water column towards the bottom, it is being degraded through a series of metabolic processes that release the nutrients bound within it. Degradation continues in the sediment, and released nutrients can now give rise to new primary production either in the water column or on the sediment surface.
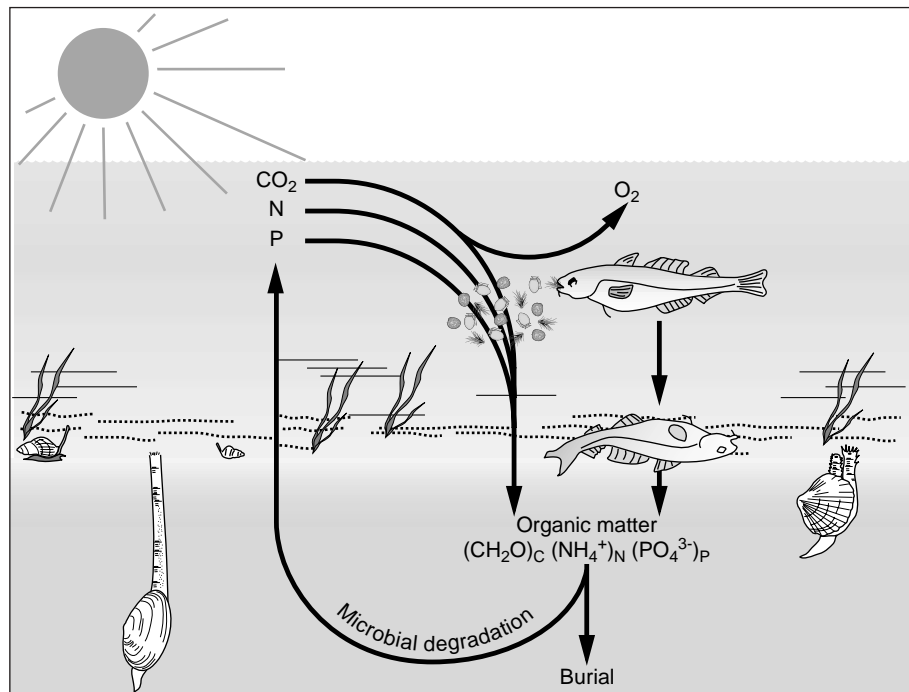
Figure 1.1. An overview of the nutrient cycle. Planktonic algae take up carbon dioxide (CO_2) through photosynthesis and convert it, together with nitrogen (N) and phosphorus (P), to organic matter. Sooner or later a portion of this organic matter reaches the sediment where it undergoes microbial degradation or is buried permanently. Through degradation CO_2, N and P are released and escape to the water column to re-enter organic matter production.

Above all, the degradation of organic matter requires oxygen, and the more material that is degraded in the water column and the sediment, the more oxygen is consumed in the process. A large organic load may therefore reduce oxygen conditions in the bottom water to a degree that oxygen depletion sets in, and the oxygen content of the upper few millimetres of the sediment may become so low that virtually all nutrient cycling takes place by anaerobic processes.

The portion of (primary) production that reaches the seabed together with other organic material mainly affects the sediment's oxygen uptake, but the exchange (or flux) of nitrogen and phosphorus across the sediment-water interface is also indirectly affected. Of course, this effect depends on season and on weather conditions in general, but monitoring nutrient fluxes and sediment oxygen uptake over several years by performing routine measurements provides a good picture of the changes, if any, occurring in the marine environment.

Below we give a thorough introduction to the sediment processes on which the model is based and the coupling between them which makes up what is known as nutrient cycling. The oxygen and nutrient flux model *per se* is described in Chapter 2.

1.1   Primary production and organic loading to the seabed

The synthesis of organic matter (primary production) takes place, as we know, through photosynthesis, which, in its simplest form, can be described as:

$$CO_2 + H_2O \rightarrow CH_2O + O_2$$
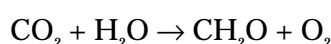
During production of organic matter, nitrogen (N) and phosphorus (P) are "built" into the organic molecules in varying ratios. Thus, the process of primary production can be described more adequately as

$$c CO_2 + N NH_4^+ + P PO_4^{3-} + C CH_2O \rightarrow (CH_2O)_C(NH_4^+)_N(PO_4^{3-})_P + c CO_2$$
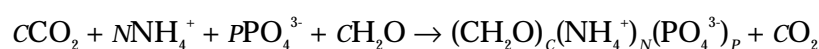
where *C*, *N* and *P* specify the number of carbon, nitrogen and phosphorus atoms, respectively, that are incorporated into the organic compound. The N and P content of the organic matter may also, like it is in the model (see Chapter 2), be presented in relation to carbon content:

$$(CH_2O)(NH_4^+)_{1/(C:N)}(PO_4^{3-})_{1/(C:P)} \text{ corresponding to } (CH_2O)_C(NH_4^+)_N(PO_4^{3-})_P$$

Sooner or later, organic matter produced through photosynthesis is degraded. During degradation of organic matter carbon is released as CO_2, and nitrogen and phosphorus as ammonium (NH_4^+) and phosphate (PO_4^{3-}), respectively, (Figure 1.1). This degradation, or cycling, or mineralisation, is photosynthesis in reverse when oxygen is present in the surrounding environment. Under oxygen depleted (anoxic) conditions consumption of nitrate, oxidised iron and manganese compounds or sulphate replaces oxygen consumption.

Degradation begins already in the water column where dead organic material is attacked by microorganisms and bacteria as it sinks towards the bottom. Microorganisms excrete hydrolytic enzymes that decompose the organic macromolecules (carbohydrates, proteins and fat) into smaller organic compounds. Bacteria are able to take up these smaller compounds through their cell membrane for use in cell metabolism, in which the organic matter is degraded and carbon, nitrogen and phosphorus released. Distance is not the only factor

determining the amount of organic matter that is degraded before it reaches the bottom. Several factors play an important part in organic loading to the seabed, such as the water's oxygen concentration and bacterial density and the amount of organic material present in the water column.

In the following sections we use examples, e.g. from Aarhus Bay, to describe how the degradation of organic matter proceeds in the seabed under oxic as well as anoxic conditions, the fate of the many chemical compounds formed, and the resultant movement of the nutrients N and P between sediment and water column.

1.2 Degradation of organic material through bacterial respiration (primary reactions)

The chemical processes that degrade organic matter and re-form CO_2, NH_4^+ and PO_4^{3-} – the molecules incorporated into the organic material through photosynthesis (Figure 1.1) – are known as the primary reactions. The primary reactions share the characteristic of taking place through bacterial respiration – in other words, these processes are all biological. The primary reactions thus differ from most of the secondary reactions, as we shall see later on.

As long as oxygen is present, organic matter degradation takes place by bacterial respiration with oxygen, also known as aerobic respiration. Oxygen is typically present in the water column and in the uppermost millimetres of the sediment, and when oxygen is depleted, mineralization continues to proceed through anaerobic respiration (i.e. respiration without oxygen). The respiration processes are distributed in a characteristic vertical pattern within the seabed. Respiration with oxygen takes place in the uppermost few millimetres of the sediment, followed by respiration with nitrate, oxidised iron and manganese compounds and sulphate, respectively (Figure 1.2). Furthest down in the sediment the degradation of organic material takes place through fermentation, by which methane is formed. In the oxygen and nutrient flux model we let the respiration processes use up the respective respiratory substrates in the order indicated above. In that way, the different respiration processes will align in more or less distinct depth intervals within the sediment.

In winter, when organic matter degradation is at its lowest, oxygen penetrates about 5 mm into the sediment of Aarhus Bay, and in summer, generally about 1-2 mm. Nitrate penetrates slightly deeper into the seabed than oxygen, and also disappears within the upper few millimetres. Oxidised manganese and iron compounds penetrate to slightly below the nitrate zone. Sulphate penetrates as far as 1-4 m into the sediment depending on organic load (Figure 1.2).

In a typical Danish marine water body such as Aarhus Bay, oxygen consuming bacteria degrade less than half of the organic material that reaches the seabed. Anaerobic bacteria take care of the remainder of the organic material – unless it is buried deeper in the sediment before degradation is complete. Of the anaerobic degradation

processes bacterial respiration with sulphate (sulphate reduction) is the most important. In Aarhus Bay, approximately 60 % of anaerobic degradation takes place through sulphate reduction, while virtually all the rest takes place through iron respiration (i.e. by bacteria utilising iron hydroxide, FeOOH, as a respiratory substrate). Compared with oxygen, sulphate and iron respiration, respiration with nitrate (denitrification) is of no great quantitative importance in the marine environment when it comes to degradation of organic matter. The denitrification process is, however, of great importance in the removal of nitrogen from the system, which will be discussed below.
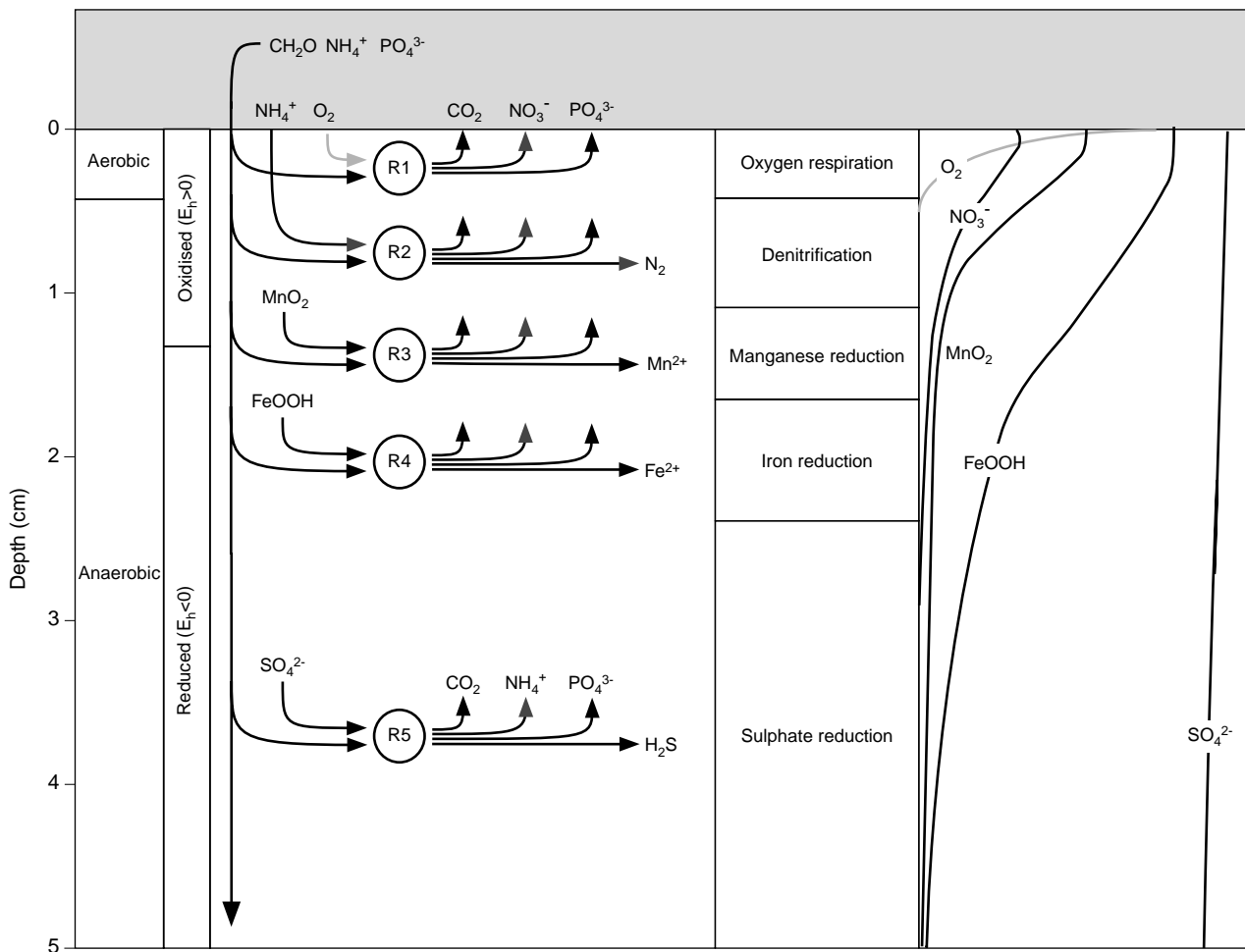
Figure 1.2. Distribution of the degradation/respiration processes in the sediment of seas and estuaries. Aerobic respiration is oxygen consuming (R1), while all other processes are anaerobic, i.e. respiration proceeds without oxygen. Here, nitrate (R2), manganese oxide (R3), iron hydroxide (R4) or sulphate (R5) act as respiratory substrates. Thus, in theory, the seabed can be divided into several zones, each of which is dominated by one of the separate processes: Oxygen respiration, denitrification, manganese reduction, iron reduction and sulphate reduction. In the right-hand panel the typical distribution of respiratory substrates in Danish coastal sediments is shown. Note that the concentrations of the individual respiratory substrates are not drawn to scale.

Apart from availability of respiratory substrates, the amount of organic matter that is actually degraded in the sediment of seas and estuaries depends on the amount and degradability of the organic matter reaching the bottom. Incompletely degraded organic matter is buried or deposited in the sediment together with the nutrients bound within it, and thus disappears from the nutrient cycles.

It is characteristic of respiration processes that they release energy for metabolic processes by transferring one or more electrons from a high-energy chemical compound to a more low-energy compound. When organic matter is degraded, it is always the carbon atoms that release electrons (e^-) and are oxidised to CO_2 in the process.

$$CH_2O + H_2O \rightarrow CO_2 + 4e^- + 4H^+$$
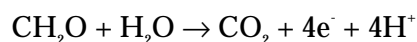
At the same time, N and P incorporated into the organic compounds via photosynthesis are released as the inorganic (nutrient) salts ammonium (NH_4^+) and phosphate (PO_4^{3-})

$$(CH_2O)_C(NH_4^+)_N(PO_4^{3-})_P + cH_2O \rightarrow$$
$$cCO_2 + NNH_4^+ + PPO_4^{3-} + 4Ce^- + 4CH^+$$
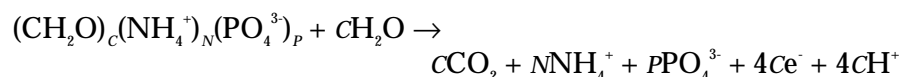
Thus, regardless of whether the respiration process is aerobic or anaerobic, CO_2, NH_4^+ and PO_4^{3-} are released. In the respiration process, either oxygen, nitrate, oxidised manganese or iron, or sulphate takes up the released electrons and is thus reduced. In the process many different "waste products", i.e. reduced chemical compounds, are formed in the sediment, e.g. reduced manganese, reduced iron and hydrogen sulphide.

In the following sections numbers in parentheses refer to the chemical reactions integrated in the mathematical model (Chapter 2; Table 2.1). For the sake of stoichiometry organic material is designated CH_2O in all chemical equations in this chapter.

1.2.1 Respiration with oxygen (aerobic respiration)

Bacteria produce carbon dioxide and water through aerobic degradation of organic material in a process that is exactly the reverse of photosynthesis.

$$O_2 + CH_2O \rightarrow CO_2 + H_2O \tag{R1}$$

As shown in Figure 1.3 the sediment oxygen uptake in Aarhus Bay varies throughout the year. The sediment oxygen uptake shown in the figure indicates the amount of oxygen consumed by bacteria for respiration (R1) as well as the amount of oxygen consumed by many of the secondary reactions presented in section 1.3. It is not technically possible to perform measurements that distinguish between the different oxygen consuming sediment processes. In Aarhus Bay oxygen consumption was high in the spring months following the onset of primary production in March and the sedimentation of new supplies of organic material. During the remainder of the year, oxygen consumption was lower due to a decrease in bottom-water oxygen content and in the amount of fresh organic material in the upper millimetres of the sediment.
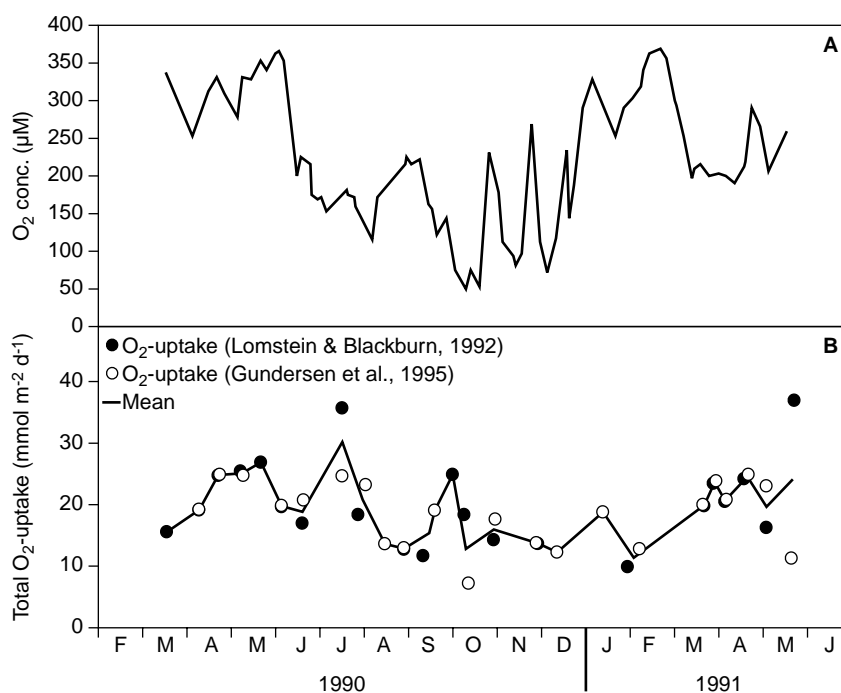
Figure 1.3. Aarhus Bay, March 1990-May 1991. A: Bottom-water oxygen concentration (measured by the County of Aarhus). B: Sediment oxygen uptake (data from Gundersen *et al.* (1995) and Lomstein & Blackburn (1992)) Note that the mean value represents the average of two measurements when these were made within one week.

1.2.2 Respiration with nitrate (denitrification)

Through anaerobic nitrate respiration denitrifying bacteria produce atmospheric nitrogen, carbon dioxide and water (Figure 1.2).

$$4NO_3^- + 5CH_2O + 4H^+ \rightarrow 2N_2 + 5CO_2 + 7H_2O \tag{R2}$$

N_2 formed in the process disappears into the atmosphere and thus ceases to present a burden to the marine environment.

It goes without saying that the presence of NO_3^- is required for the denitrification process to take place. Nitrate for denitrification may come from the bottom water or be formed in the sediment by oxidation of NH_4^+ to NO_3^-. We will save the description of NH_4^+ oxidation until we reach the section on secondary reactions, but we can reveal now that this process requires the presence of oxygen. In other words, even if there is no NO_3^- in the bottom water, denitrification can still proceed. As long as the sediment contains oxygen, NO_3^- can be formed by oxidation of NH_4^+. And there is always plenty of ammonium to be found in the seabed. In Aarhus Bay there is virtually no NO_3^- in the bottom water in summer and at the same time the oxygen concentration is very low. Therefore, the denitrification activity is markedly reduced in this period (Figure 1.4). During autumn when the bottom-water oxygen concentration becomes higher, the production of NO_3^- resumes and together with bottom-water NO_3^- this causes the denitrification activity to increase.

14
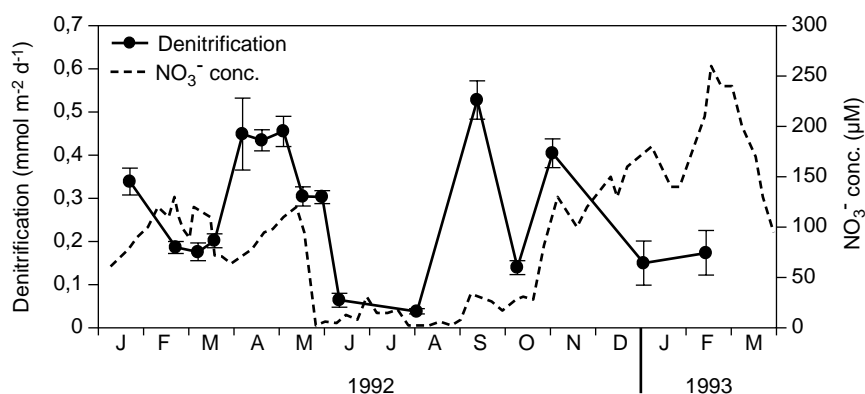
Figure 1.4. Nitrate concentrations and denitrification in Aarhus Bay January 1992-March 1993. Concentrations of nitrate were measured by the County of Aarhus. Denitrification rates ± SE (n=3) from Nielsen *et al.* (1994).

1.2.3   Respiration with manganese and iron

Through respiration with manganese oxide, manganese-reducing bacteria produce dissolved, reduced manganese, carbon dioxide and water (Figure 1.2).

$$2MnO_2 + CH_2O + 4H^+ \rightarrow 2Mn^{2+} + CO_2 + 3H_2O \qquad (R3)$$

As opposed to transport of particulate manganese oxide, which takes place via bioturbation, the transport of Mn^{2+} is diffusive. In its oxidised form, manganese reacts with H_2S to form Mn^{2+}, whereas reduced manganese is oxidised rapidly to MnO_2 in the presence of oxygen, as we will discuss later.

During anaerobic bacterial respiration with iron hydroxide dissolved, reduced iron, carbon dioxide and water are formed (Figure 1.2).

$$4FeOOH + CH_2O + 8H^+ \rightarrow 4Fe^{2+} + CO_2 + 7H_2O \qquad (R4)$$
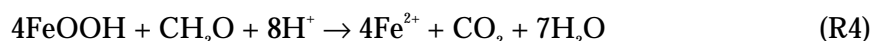
As in the case of manganese, iron in its oxidised form is a particulate material, while being soluble in its reduced form. Reduced iron reacts spontaneously with both MnO_2 and O_2 to form FeOOH. By reaction of Fe^{2+} with H_2S a precipitate of particulate iron sulphide (FeS) is formed, which turns the sediment black. These secondary reactions will be discussed later.

It is technically very difficult to measure bacterial respiration with manganese and iron. Therefore, seasonal investigations of these respiration processes have yet to be performed in Aarhus Bay – and anywhere else in the world for that matter. In Aarhus Bay the importance of the two respiration processes has in fact been determined on a few occasions, and these measurements indicate that bacterial manganese respiration is of marginal importance to organic matter degradation in Aarhus Bay, while iron respiration accounts for about 20 % of total degradation.

15

1.2.4 Respiration with sulphate (sulphate reduction)

Sulphate reducing bacteria use sulphate as a respiratory substrate, and through this anaerobic respiration process hydrogen sulphide, carbon dioxide and water are produced (see Figure 1.2)

$$SO_4^{2-} + 2CH_2O + 2H^+ \rightarrow H_2S + 2CO_2 + 2H_2O \qquad (R5)$$

Hydrogen sulphide is an evil-smelling and highly poisonous waste product. Through secondary reactions H_2S is removed from the seabed, either by reaction with the oxidised compounds O_2, MnO_2 and $FeOOH$, or as an iron-sulphide precipitate formed by reaction with Fe^{2+}. These processes are discussed in the following section.

The annual variation in sulphate reduction is shown in Figure 1.5. Sulphate reduction rates peak in summer and autumn at which time temperatures in the seabed are also at their highest. As bottom-water temperatures fall, respiration with sulphate slows down, and this is why sulphate reduction rates are lowest in winter.
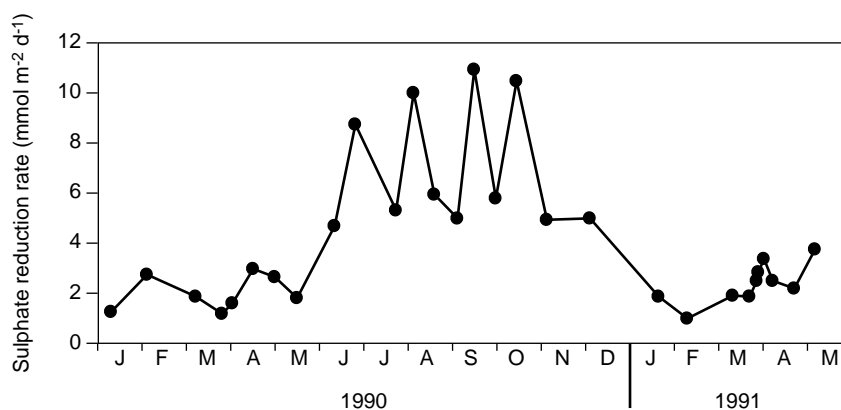
Figure 1.5. Sulphate reduction rates in Aarhus Bay January 1990-May 1991. Based on measurements by Fossing *et al.* (1992).

1.2.5 Methane production (methanogenesis)

Deepest down in the sediment, below the sulphate zone, methane is produced by fermentation of organic material: $2CH_2O \rightarrow CH_4 + CO_2$. Organic matter degradation through methanogenesis is of no importance to nutrient cycling in the upper part of the seabed in Aarhus Bay, and will be discussed no further. For the same reason, the process is not included in the model.

1.3 Decomposition of bacterial degradation products (secondary reactions)

In contrast to primary reactions, which are all bacterial respiration processes, most secondary reactions are purely chemical. In the previous section we saw that bacterial degradation of organic matter leads to release of a number of metabolic products; CO_2 and H_2O as well as the nutrients NH_4^+ and PO_4^{3-} and a series of waste products; N_2 (through denitrification), Mn^{2+} (through manganese respiration), Fe^{2+} (through iron respiration) and H_2S (through sulphate reduction), see

Figure 1.2. One might say that the secondary reactions deal with these products and restore the respiration substrates, e.g. NO_3^-, MnO_2, FeOOH and SO_4^{2-}. Through diffusion the products CO_2 and N_2 move from the sediment into the sea water where both gasses are in equilibrium with the atmosphere. As neither carbon dioxide nor atmospheric nitrogen enter into chemical processes that may disrupt the model, they will not be discussed further. Decomposition of the remaining metabolic products is outlined in the following.

1.3.1 Nitrate (NO_3^-) and ammonium (NH_4^+)

Nitrifying bacteria are able to release the energy bound in NH_4^+ by oxidising it to NO_3^-. When bacteria oxidise ammonium to nitrate, oxygen serves as electron acceptor.

$$NH_4^+ + 2O_2 \rightarrow NO_3^- + H_2O + 2H^+ \tag{R6}$$
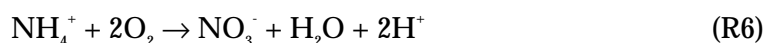
Thus, the nitrification process takes place only in the presence of oxygen, i.e. in the upper few millimetres of the sediment and around polychaete tubes etc., where oxygen may be transported deeper into the sediment, for instance by irrigation (Figure 1.6). In other words, ammonium produced through organic matter degradation in oxygen-free zones within the sediment must diffuse towards the sediment surface or a polychaete tube in order for NH_4^+ to encounter oxygen and be oxidised to NO_3^-. In situations where the seabed is subject to oxygen deficiency or oxygen depletion NH_4^+ diffusion may become so intense that NH_4^+ escapes to the bottom water from the sediment surface or is expelled from polychaete tubes.
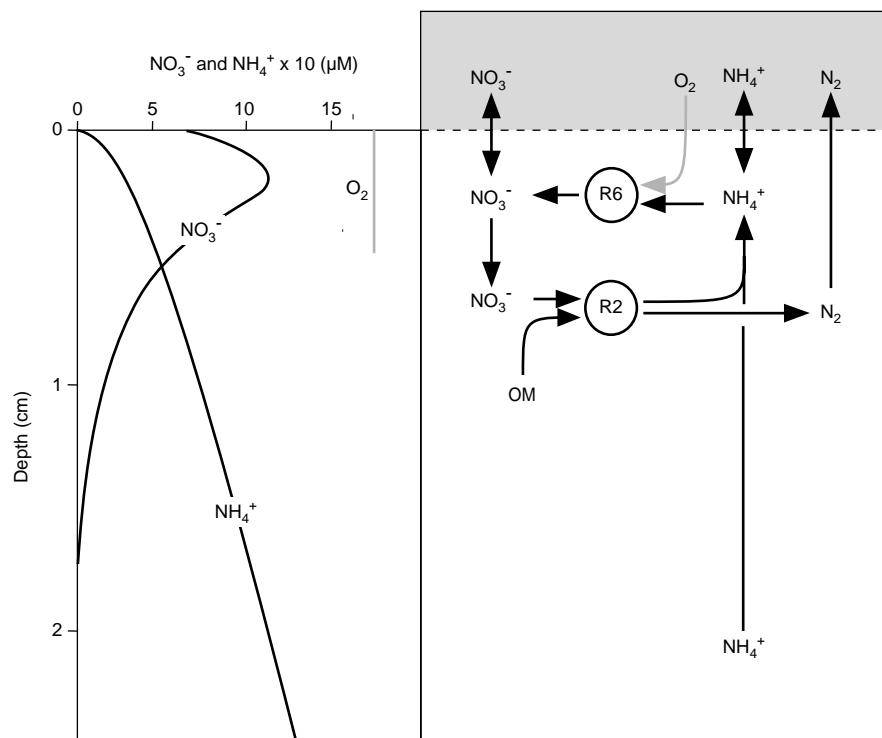
Figure 1.6. The nitrogen cycle (simplified) Typical NO_3^- and NH_4^+ concentrations in the upper 2.5 cm are shown together with the thickness of the oxygen containing surface layer. OM designates organic matter: $(CH_2O)_C(NH_4^+)_N(PO_4^{3-})_P.$ Please refer to the text for information on reactions R2 and R6.

As in the case of NH_4^+, exchange of NO_3^- may take place between sediment and bottom water. The direction of the nitrogen flux is governed by concentration gradients across the sediment/bottom water interface. Once the nitrogen (nutrient) salts have entered the seawater, both benthic and pelagic plankton and other primary producers may take them up and incorporate them into organic material through photosynthesis.

In winter and spring, favourable oxygen conditions in the sediment stimulate the nitrification process. Thus, at this time of the year an increased export of nitrate out of the seabed is often observed (Figure 1.7). As summer proceeds and the oxygen content declines, nitrification decreases as well. On the other hand, the flux of ammonium out of the sediment increases, and in this period NH_4^+ may be the dominant nitrogen species being exported to the water column (Figure 1.8). Nitrogen exchange between sediment and water column is the result of a complex equilibrium governed by a series of factors such as organic load to the sediment, temperature and the water-column content of oxygen, ammonium and nitrate.
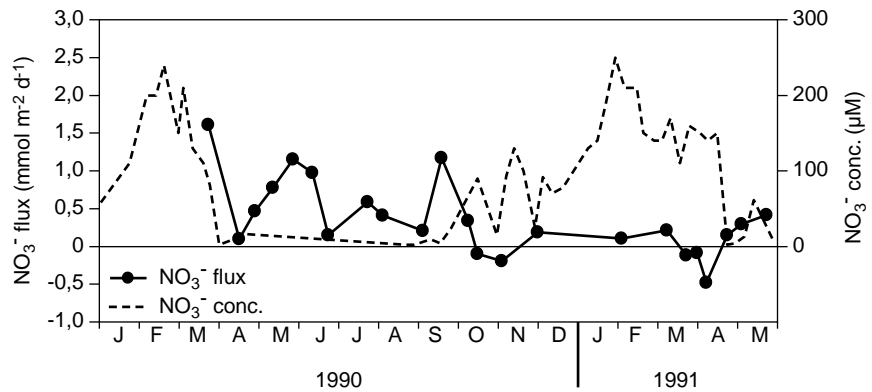
Figure 1.7. Nitrate concentrations and nitrate flux in Aarhus Bay January 1990-May 1991. Nitrate concentrations were measured by the County of Aarhus. Data on nitrate flux from Lomstein & Blackburn (1992).
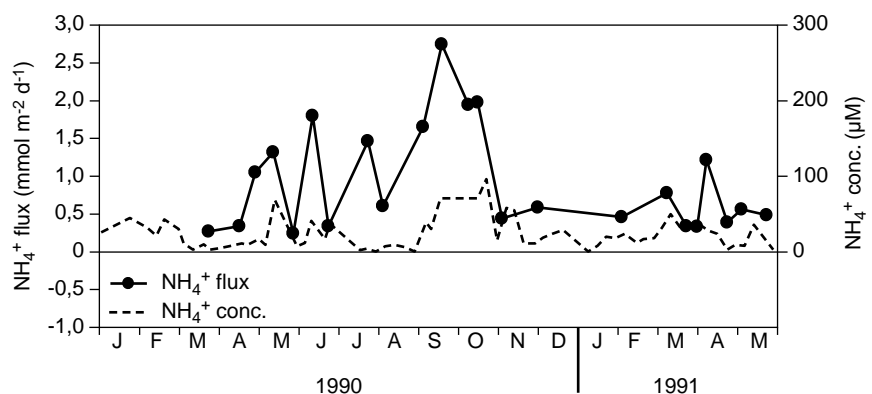
Figure 1.8. Ammonium concentrations and ammonium flux in Aarhus Bay January 1990-May 1991. Ammonium concentrations were measured by the County of Aarhus. Data on ammonium flux from Lomstein & Blackburn (1992).

1.3.2 Phosphate (PO_4^{3-})

Through mineralisation, phosphorus is released as inorganic phosphate. In contrast to all other chemical compounds in the marine environment phosphorus retains its oxidation level. In other words the phosphorus atom invariably occurs at oxidation level +5 in the form of orthophosphate, PO_4^{3-}. Depending on concentration gradients, phosphate, like nitrate and ammonium, diffuses to and from sediment and bottom water, but unlike NH_4^+, PO_4^{3-} is bound tightly within the sediment under certain oxidative conditions. Phosphate is bound within the sediment to oxidised iron compounds, among others. The bond is indicated by $\equiv$ in the chemical equation

$$(FeOOH)_N + PO_4^{3-} \rightarrow (FeOOH)_N\equiv PO_4^{3-} \tag{R7}$$

As we shall see in the following section, the sediment releases its "iron grip" on the phosphate molecule the moment FeOOH is reduced to Fe^{2+}, because the complex dissolves, and PO_4^{3-} is immediately free to diffuse into the bottom water as long as the concentration gradient allows it (Figure 1.9). Primary producers in the seawater and on the sediment surface are ever ready to assimilate the released phosphate and incorporate it into organic material through photosynthesis, if light conditions are sufficiently favourable.

The environmental conditions and reaction mechanisms influencing iron-bound phosphorus will be discussed in the section on iron.
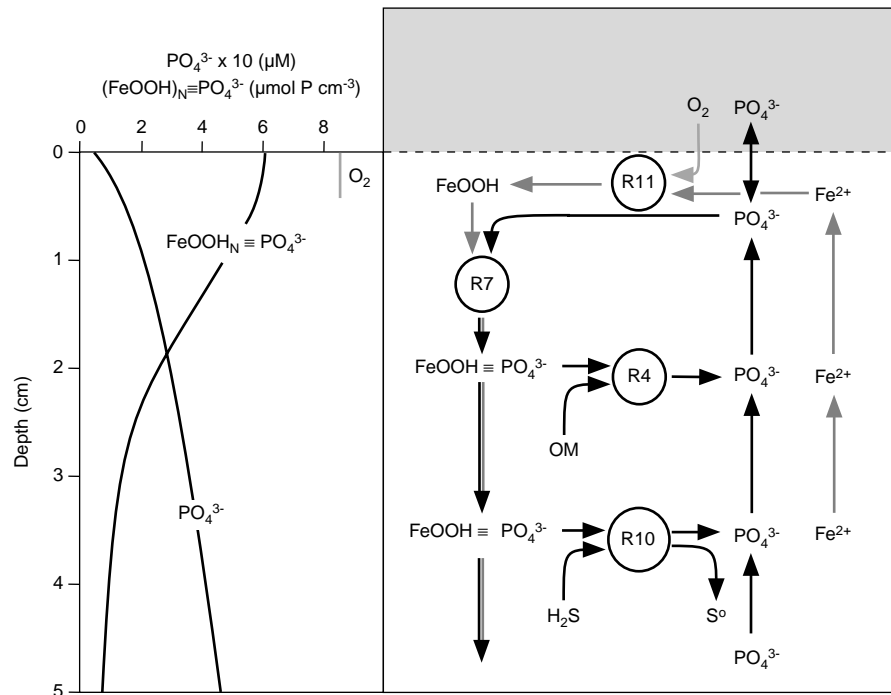
Figure 1.9. The phosphorus cycle (simplified) Typical PO_4^{3-} and $(FeOOH)_N\equiv PO_4^{3-}$ (iron-bound phosphate) concentrations in the upper 5 cm of the sediment are shown together with the thickness of the oxygen containing surface layer. The part of the iron cycle overlapping the phosphorus cycle is indicated by grey print. R10 designates the impact of the sulphur cycle on $(FeOOH)_N\equiv PO_4^{3-}$. OM designates organic matter $(CH_2O)_C(NH_4^+)_N(PO_4^{3-})_P$. Please refer to the text for information on reactions R4, R7, R10 and R11.

1.3.3 Manganese oxide (MnO_2) and dissolved reduced manganese (Mn^{2+})

As when manganese-reducing bacteria use particulate manganese oxide as a respiration substrate (see R3), Mn^{2+} is formed when MnO_2 reacts with Fe^{2+}

$$2Fe^{2+} + MnO_2 + 2H_2O \rightarrow 2FeOOH + Mn^{2+} + 2H^+ \qquad (R8)$$
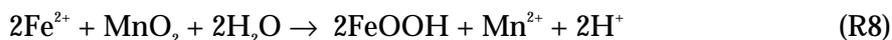
When Mn^{2+} formed by reduction encounters oxygen, it is oxidised to MnO_2 once again.

$$2Mn^{2+} + O_2 + 2H_2O \rightarrow 2MnO_2 + 4H^+ \qquad (R9)$$
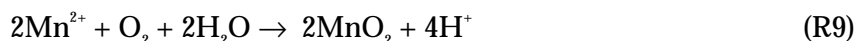
The process takes place mainly immediately below the sediment surface where Mn^{2+} precipitates rapidly in the form of manganese oxide in the presence of oxygen. The role of manganese oxide in the sediment of Aarhus Bay is presumed to be insignificant in regard to oxidation of Fe^{2+} (R8) and oxygen consumption (R9).

Animals that pump water into and out of the seabed (irrigation) also affect Mn^{2+} concentrations within the sediment, partly by removing Mn^{2+} and partly by causing oxygen to penetrate slightly deeper into the sediment than would be the case by diffusion alone. We will
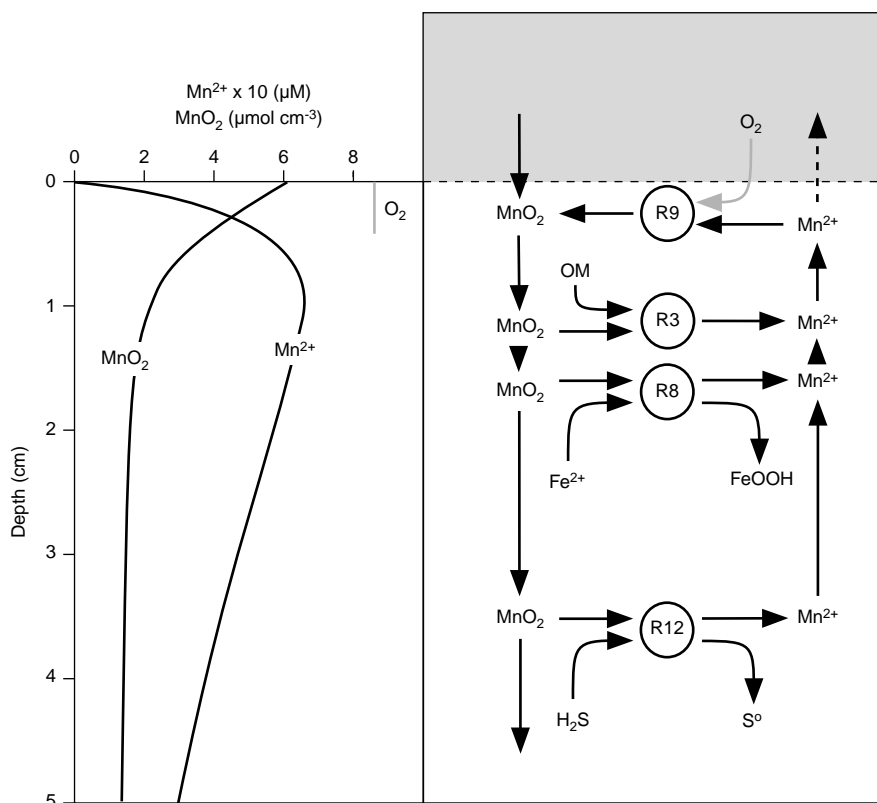
Figure 1.10. The manganese cycle (simplified) Typical MnO_2 and Mn^{2+} concentrations in the upper 5 cm of the sediment are shown together with the thickness of the oxygen containing surface layer. The parts of the manganese cycle overlapping the iron and sulphur cycles are indicated by R8 and R12, respectively. OM designates organic matter $(CH_2O)_C(NH_4^+)_N(PO_4^{3-})_P$. Please refer to the text for information on reactions R3, R8, R9 and R12.

discuss the importance of irrigation and bioturbation in relation to nutrient cycling towards the end of this chapter.

1.3.4 Particulate oxidised iron (FeOOH) and dissolved reduced iron (Fe^{2+})

The brownish colour often seen in the surface layer of the sediment, is caused by oxidised iron compounds that are found in particulate (immobile) form in the upper few centimetres of the seabed, i.e. in and immediately below the oxidised zone. As mentioned earlier, iron-reducing bacteria use oxidised iron as a respiration substrate in the degradation of organic matter (R4). However, the ecological role of oxidised iron compounds in retaining phosphate within the seabed is no less significant (Figure 1.9 and R7). When iron-reducing bacteria reduce FeOOH, bound phosphate is released. Phosphate release also takes place through a non-biological reaction of hydrogen sulphide with FeOOH

$$nH_2S + 2(FeOOH)_N \equiv PO_4^{3-} + 4NH^+ \rightarrow nS^o + 2nFe^{2+} + 4nH_2O + 2PO_4^{3-} \tag{R10a}$$
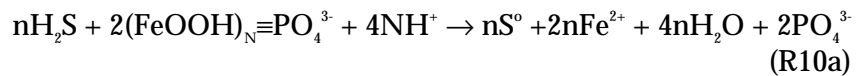
Reduced iron (Fe^{2+}) is immediately converted into FeOOH if it encounters O_2, e.g. in the oxidised zone of the seabed, or escapes to the bottom water.

$$4Fe^{2+} + O_2 + 6H_2O \rightarrow 4FeOOH + 8H^+ \tag{R11}$$
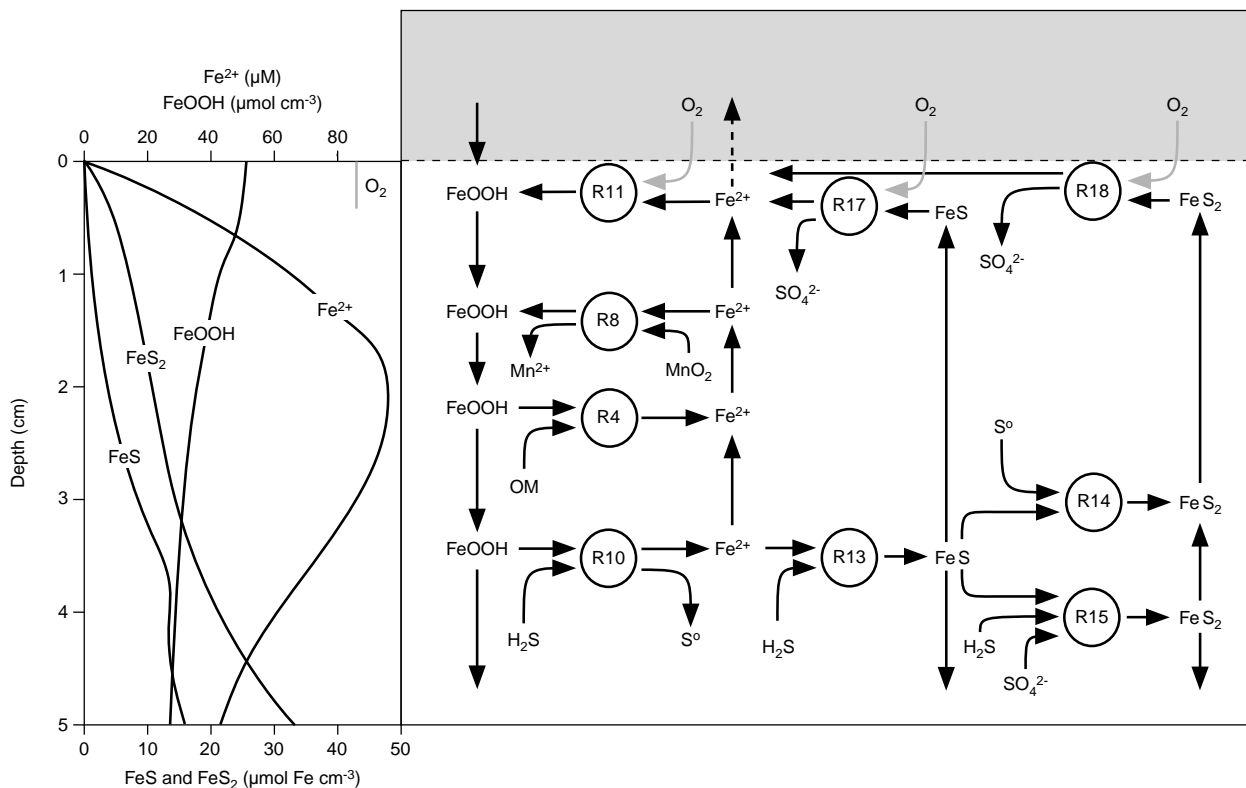
Figure 1.11. The iron cycle (simplified) Typical FeOOH, Fe^{2+}, FeS and FeS_2 concentrations in the upper 5 cm of the sediment are shown together with the thickness of the oxygen-containing surface layer. The part of the iron cycle overlapping the manganese cycle is indicated by R8, while overlaps with the sulphur cycle are indicated by R10, R13, R14, R15, R17 and R18. OM designates organic matter $(CH_2O)_C(NH_4^+)_N(PO_4^{3-})_P$. Please refer to the text for information on "R" reactions.

Like manganese oxide, iron reacts with hydrogen sulphide as discussed in the following section.

1.3.5 Sulphate (SO_4^{2-}), hydrogen sulphide (H_2S), particulate sulphur (S^o) and iron sulphides (FeS and FeS_2)

As we have seen, hydrogen sulphide is the respiration product of organic matter degradation by sulphate reducing bacteria. H_2S production takes place in the reduced zone of the sediment, and from this zone H_2S diffuses towards the sediment surface (Figure 1.12). Before hydrogen sulphide reaches the oxidised sediment zone, oxidised iron or manganese compounds may oxidise H_2S to particulate sulphur, or H_2S may be temporarily bound within the sediment as particulate iron sulphide (FeS).

$$H_2S + 2FeOOH + 4H^+ \rightarrow S^o + 2Fe^{2+} + 4H_2O \qquad \text{(R10b)}$$
$$H_2S + MnO_2 + 2H^+ \rightarrow S^o + Mn^{2+} + 2H_2O \qquad \text{(R12)}$$
$$H_2S + Fe^{2+} \rightarrow FeS + 2H^+ \qquad \text{(R13)}$$
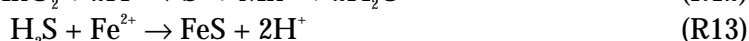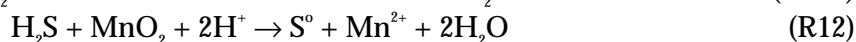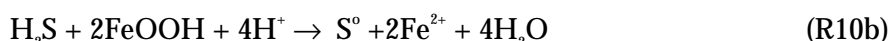
Some of the iron sulphide reacts with particulate sulphur to form pyrite (FeS_2), which contributes to the light grey colour seen deeper within the sediment

$$FeS + S^o \rightarrow FeS_2 \qquad \text{(R14)}$$

Another important reaction path for pyrite formation is the reaction of FeS with H_2S. This process leads to formation of hydrogen (H_2) as well, which sulphate reducing bacteria remove by a mechanism
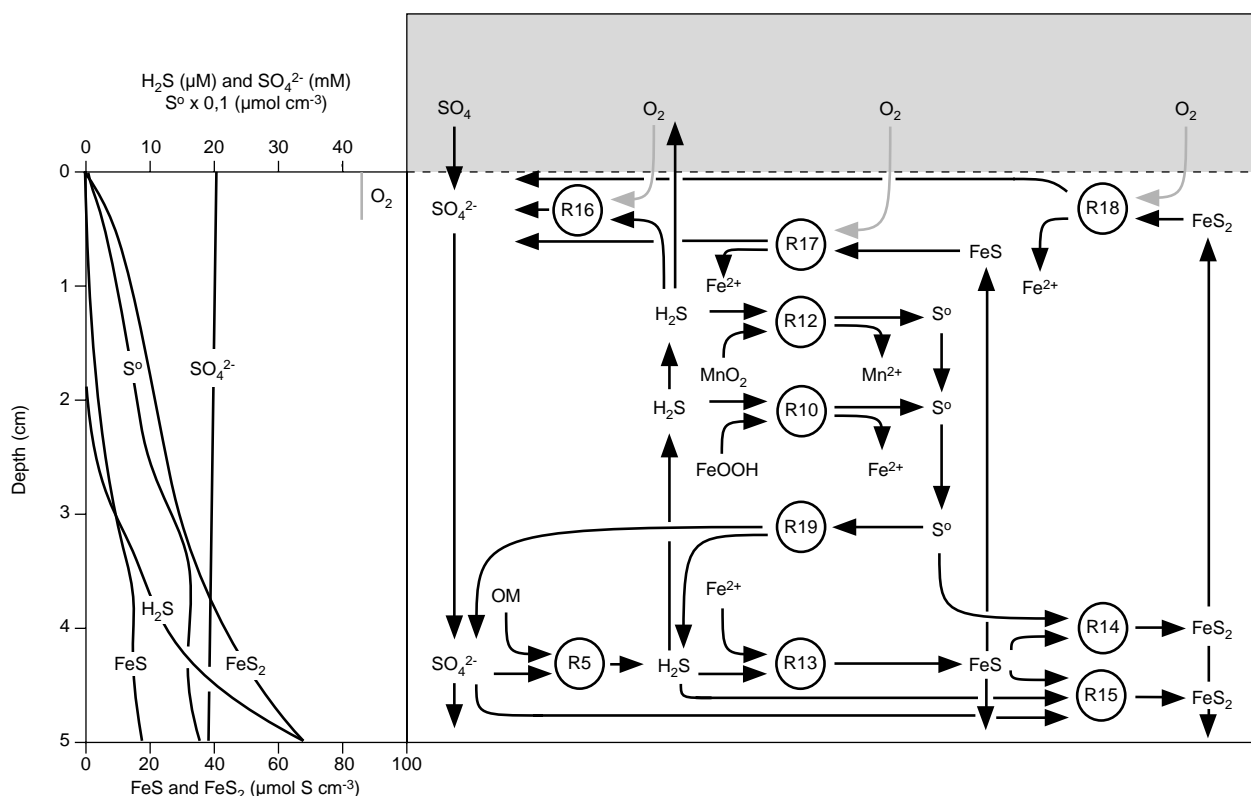
Figure 1.12. The sulphur cycle (simplified) Typical SO_4^{2-}, S^o, H_2S, FeS and FeS_2 concentrations in the upper 5 cm of the sediment are shown together with the thickness of the oxygen containing surface layer. The part of the sulphur cycle overlapping the manganese cycle is indicated by R12, while overlaps with the iron cycle are indicated by R10, R13, R14, R15, R17 and R18. OM designates organic matter $(CH_2O)_C(NH_4^+)_N(PO_4^{3-})_P$. Please refer to the text for information on "R" reactions.

analogous to their degradation of organic matter. The two processes are expressed by the gross process (R15)

$$SO_4^{2-} + 4H_2 + 2H^+ \rightarrow H_2S + 4H_2O$$
$$\underline{FeS + H_2S \rightarrow FeS_2 + H_2}$$
$$SO_4^{2-} + 3H_2S + 4FeS + 2H^+ \rightarrow 4FeS_2 + 4H_2O \qquad (R15)$$
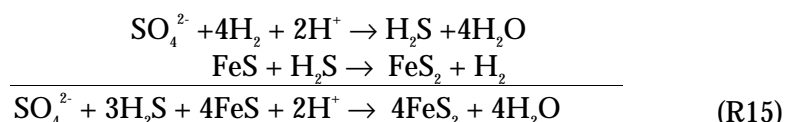
If sulphide comes into contact with oxygen in the uppermost few millimetres of the seabed, it is oxidised to sulphate, which may be utilised once again in bacterial respiration.

$$H_2S + 2O_2 \rightarrow SO_4^{2-} + 2H^+ \qquad (R16)$$
$$FeS + 2O_2 \rightarrow Fe^{2+} + SO_4^{2-} \qquad (R17)$$
$$2FeS_2 + 7O_2 + 2H_2O \rightarrow 2Fe^{2+} + 4SO_4^{2-} + 4H^+ \qquad (R18)$$

The final process of importance to the marine nutrient cycle is the transformation of the particulate sulphur that has escaped reaction with FeS (R14). When a low concentration of H_2S is maintained in the seabed due to continuous removal of hydrogen sulphide, for instance via R10, S^o is transformed through a process called disproportionation. This may be seen as a form of inorganic fermentation. In other words, particulate sulphur is both oxidised (to SO_4^{2-}) and reduced (to H_2S) through one and the same reaction.

$$4S^o + 4H_2O \rightarrow 3H_2S + SO_4^{2-} + 2H^+ \qquad (R19)$$
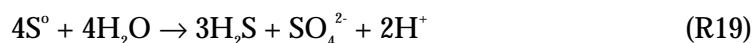
In Aarhus Bay and other coastal sediments sulphate reduction activity, and with it hydrogen sulphide production, increases as summer proceeds, peaking in late summer and early autumn when total mineralisation of organic matter is at its highest (Figure 1.5). During this period H_2S reacts with many of the oxidised iron and manganese compounds (R10 and R12) and H_2S is bound within the sediment by reaction with reduced iron (R13). In this way, the H_2S pool uses up still more of the oxidised iron and manganese pools in the seabed, and the extent of the brown (oxidised) sediment zone gradually decreases. If hydrogen sulphide uses up the entire reserve of oxidised iron and manganese compounds in the seabed during the summer months, H_2S may reach the oxygen containing sediment zone and cause significant oxygen consumption (R16). Once oxygen is gone from the sediment, H_2S is free to escape into the bottom water where oxygen depletion rapidly sets in and benthic animals begin to die from the highly poisonous hydrogen sulphide.

1.4   The carbon cycle (coupling between primary and secondary reactions)

The nitrogen, manganese, iron and sulphur cycles have in common that organic matter enters into them and that decomposition of this organic matter is the energy-providing process fuelling them. Thus, describing the nutrient cycles as though they were independent of one another is not entirely correct, but does serve to facilitate our understanding of them. Both the chemical reactions (R1-R19) and the figures describing the nutrient cycles (Figure 1.6; Figure 1.9; Figure 1.10; Figure 1.11; Figure 1.12) clearly demonstrate that many of the

chemical compounds in the seabed enter into more than one nutrient cycle. One example is oxygen. Oxygen enters not only into the degradation of organic material (R1) but into all cycles in the oxidation of several degradation products (R6, R9, R11. R16, R17 and R18).

The common denominator of organic matter degradation – the organic nutrient cycle – may thus be presented by describing all cycles (Figure 1.6; Figure 1.9; Figure 1.10; Figure 1.11; Figure 1.12) and the reactions involved (R1 to R19) in one. Of course, this produces a much more complex picture of the processes taking place in the seabed, but also, and more importantly, a far more accurate and correct description of sediment nutrient cycling (Figure 1.13). And a description such as this is just what development of the oxygen and nutrient flux model is designed to achieve.
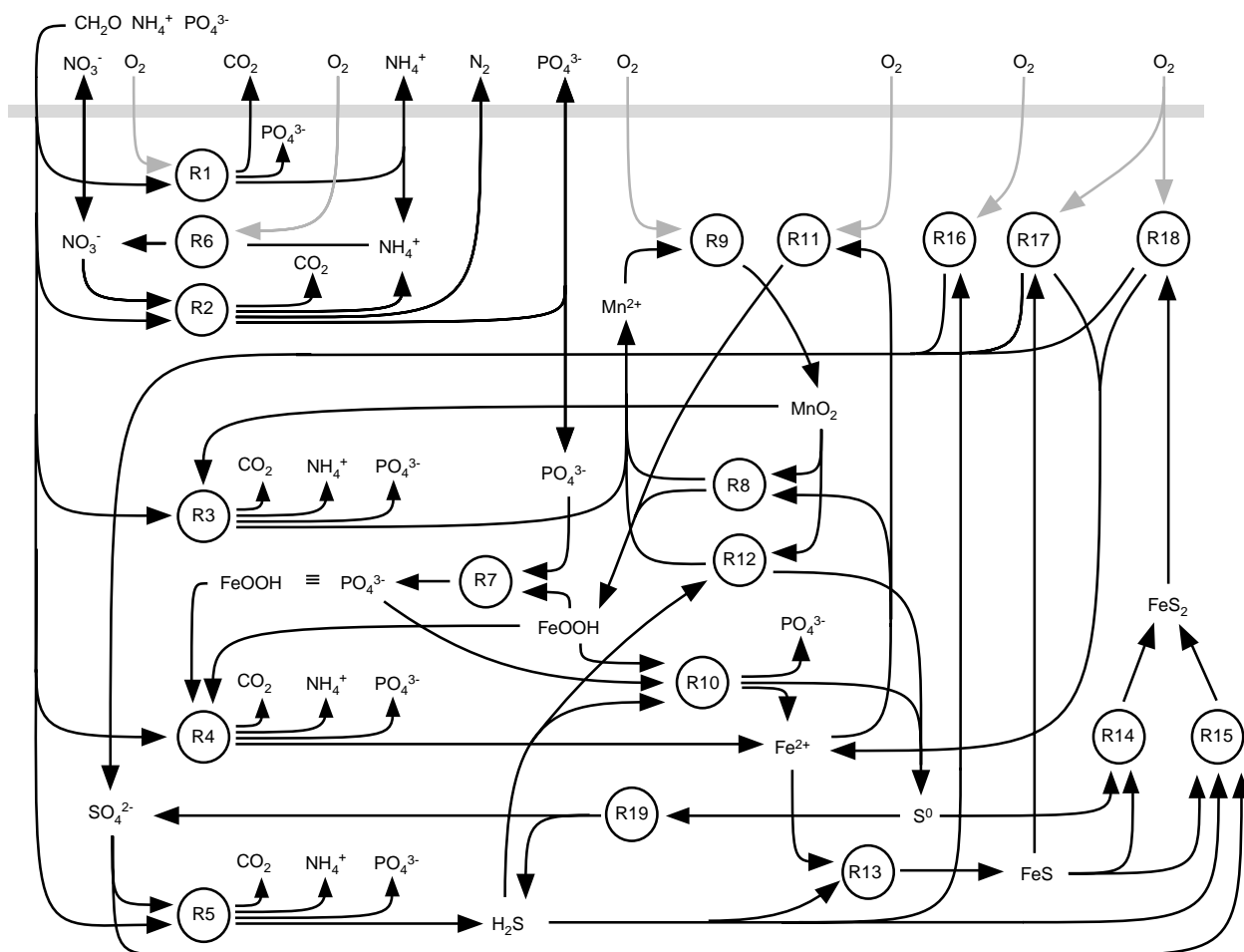
Figure 1.13. The complex relation between the nutrient cycles in sediments of seas and estuaries, comprising nitrogen (Figure 1.6), phosphorus (Figure 1.9), manganese (Figure 1.10), iron (Figure 1.11) and sulphur (Figure 1.12). The processes have in common that they directly or indirectly influence the degradation of organic matter $(CH_2O)_C(NH_4^+)_N(PO_4^{3-})_P$. The shaded bar at the top of the figure indicates the interface between sediment and bottom water. It is across this interface that CO_2 and O_2 are exchanged and the nutrients N and P released to the water column or taken up in the sediment. The intricacy depicted here provides a visual impression of the oxygen and nutrient flux model described in Chapter 2.

1.5   Bioturbation and bioirrigation

In their search for food and ideal environments, animals living in or on the seabed contribute towards thoroughly disturbing the uppermost centimetres of the sediment. The process is called bioturbation and arises from the more or less random movements of animals within the seabed. Bioturbation causes mixing not only of the sediment but also of the many chemical compounds found within the seabed. This applies to compounds dissolved in pore water (e.g. NO_3^-), solids (e.g. FeOOH) and (dissolved) compounds adsorbed to the sediment (e.g. NH_4^+).

Apart from disturbing the sediment, some bottom-dwelling animals construct tubes or channels in the sediment, thus creating a connection to the bottom water. The animals actively pump water in and out of these tubes – to feed, and to obtain fresh, oxygenated water for respiration. This pumping activity is called (bio)irrigation. When animals pump bottom water into the sediment, dissolved compounds follow, and, similarly, dissolved compounds escape from the sediment into the bottom water when water is pumped out.

Animal activity in and on the seabed is included in the oxygen and nutrient flux model. In Chapter 2 we describe how bioturbation and bioirrigation vary over the year depending on bottom-water oxygen concentrations.

1.6   The sediment's hydrogen sulphide buffering capacity, oxidation reserve and oxygen debt

The sediment's hydrogen sulphide buffering capacity, oxidation reserve and oxygen debt are environmental parameters, each in its way expressing the ability of the seabed to prevent H_2S from escaping to the bottom water and to oxidise reduced compounds within the sediment.

We have demonstrated above that hydrogen sulphide production (R5) is a significant process in the degradation of organic material. The large H_2S production seen especially in summer and autumn months (Figure 1.5) means that a correspondingly high consumption of oxygen is possible at this time of year if H_2S comes into contact with surface-sediment and bottom-water oxygen (R16). Unfortunately, increased H_2S production often coincides with low bottom-water oxygen concentrations. In other words, the stage is set for the bottom water to be stripped of the last vestiges of life-sustaining oxygen in late summer. The main reason that it does not always turn out that way, is the iron content of the sediment.

Iron in the seabed reacts with H_2S and precipitates as S^o or FeS (R10 and R13). Iron thus prevents H_2S from reaching the oxidised top layer of the sediment. This enables the seabed and the bottom water to preserve a small residue of oxygen. As long as the seabed contains sufficient iron to bind produced H_2S, only a small portion of the oxygen transported into the sediment by irrigation is used up. But when most of the iron is bound in the form of iron sulphides (FeS and

FeS_2) H_2S flows into the bottom water unchecked and oxygen rapidly disappears. If the seabed is to be able to withhold H_2S summer after summer, continuous renewal of the iron pool is required. This is secured, for instance, when FeOOH, bound during summer in FeS and FeS_2, is re-formed through oxidation (R16, R17, R8 and R11) when animals burrowing in the sediment transport reduced iron compounds to the oxygen-containing sediment layers. The iron pool may also be restored when waves or currents cause bottom material to come into contact with oxygen by disturbing the sediment surface.

The capacity of the seabed for binding hydrogen sulphide is called the sediment's hydrogen sulphide buffering capacity, sulphide buffering capacity or just buffering capacity. One may also use the term "oxidation reserve" as a way of expressing that the seabed's iron and manganese pools are in fact capable of binding H_2S and thus correspond to several months' oxygen consumption. In other words, the fact that manganese and iron bind H_2S within the sediment in the summer season merely causes the consumption of oxygen to be delayed a few months. Thus, one might say that the seabed runs up an "oxygen debt" and that this debt must be repaid in the winter season if the sediment's hydrogen sulphide buffering capacity is to be normalised by the beginning of the summer season.

It goes without saying that as the hydrogen sulphide buffering capacity and consequently the oxidation reserve declines during the summer season, the oxygen debt increases accordingly. The oxidation reserve will, of course, vary from year to year depending on the degree to which the previous year's oxygen debt was repaid and on the amount of "new" oxidised manganese and iron added to the seabed through sedimentation. It is quite simple, however, to calculate the size of the oxidation reserve (mol O_2 eq. m^{-2}) at a given point in time as long as the sediment's content of O_2, MnO_2 and FeOOH is known. The oxidation reserve can thus be expressed by the following formula:

$$O_{res} = [O_2] +\ 0.5\ [MnO_2] + 0.25\ [FeOOH]\ mol\ O_2\text{-eq.}\ m^{-2}$$

Where *[O$_2$]*, *[MnO$_2$]* and *[FeOOH]* denote the pools of oxygen and of oxidised manganese and iron in the sediment (mol m^{-2}) and *0.5* and *0.25* are factors converting MnO_2 and FeOOH, respectively, into oxygen equivalents. The oxygen content of the seabed is negligible in comparison with the pools of MnO_2 and FeOOH and of the latter two pools the manganese pool constitutes less than 5% of the iron pool. So, in practice, the oxidation reserve is dependent solely on the oxidised iron pool.

$$O_{res} \approx 0.25\ [FeOOH]\ mol\ O_2\text{-eq.}\ m^{-2}$$

As temperatures fall and the organic load to the seabed decreases during winter, mineralisation declines as well. The overall result is rising oxygen concentrations within the sediment. Improved oxygen conditions at the bottom and resuspension of surface sediment causes Mn^{2+}, Fe^{2+}, H_2S, FeS and FeS to be oxidised to a certain degree through consumption of oxygen (see R9, R11, R16, R17 and R18). Only then is

a significant portion of the oxygen debt (generated during summer through production of H_2S) repaid. Popularly speaking, the oxidised iron (and manganese) pool was able to delay the actual oxygen consumption by oxidising or precipitating with the produced hydrogen sulphide. The pool of oxidised iron, which is the dominant compound, puts a "lid" or draws an "iron curtain", so to speak, on the reduced sediment and temporarily "swallows" the oxygen consumption required especially by the oxidation of hydrogen sulphide. Thus, the cascade of oxidation and reduction processes initiated by the oxidation of hydrogen sulphide is halted for a time by oxidised iron and is not triggered before reduced iron compounds are oxidised through sediment resuspension brought on by the vigorous autumn storms (Figure 1.14).
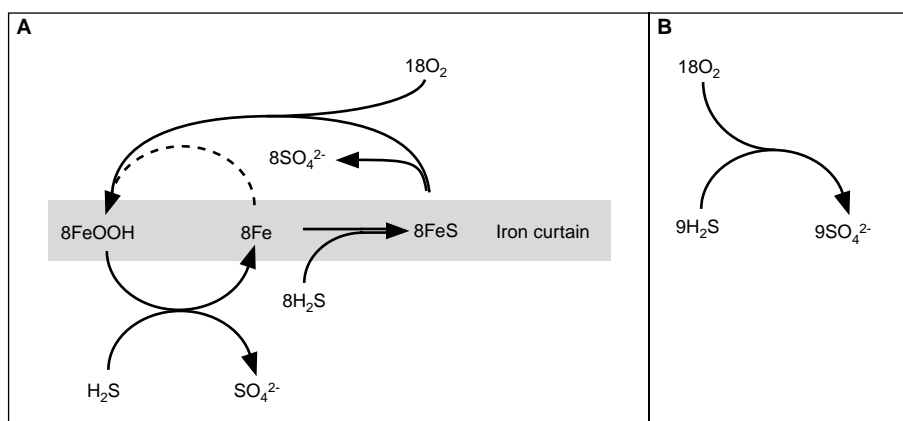
Figure 1.14. The effective barrier warding off hydrogen sulphide release is called the iron curtain. A: Iron hydroxide (FeOOH) reacts effectively with H_2S and is reduced to Fe^{2+}, which precipitates rapidly with H_2S as black iron sulphide (FeS). Much later, oxygen oxidises FeS to FeOOH and SO_4^{2-}. B: Without the iron curtain H_2S is not bound within the sediment but reacts immediately with O_2, and no delay in the oxidation of H_2S is seen. Note that the amount of oxygen required for oxidation of 8 mol FeS and 9 mol H_2S, respectively, is exactly the same: 18 mol O_2.

[Blank page]

2 Construction and functioning of the sediment flux model

In Chapter 1 we described the degradation of organic material via bacterial respiration and the various respiration substrates: oxygen, nitrate, oxidised manganese and iron compounds and sulphate. We called these processes the primary reactions. We also described the decomposition of nutrients and the many waste products through what we called the secondary reactions. In this chapter we will process this knowledge and use it to construct a (mathematical) model describing the interrelationship between the many primary and secondary reactions taking place in the sediment. Because of the interdependency of the many processes an "all-encompassing" model such as this is a unique and necessary tool if you want to gain a quantitative understanding of how the exchange of nutrients between sediment and bottom water is governed by the interactions of biological and chemical processes and by solute and particle transport within the sediment. The skeleton of the model is made up of the hundreds of data and observations obtained in Aarhus Bay 1990-91 in connection with the Marine Research Programme 1990 (HAV90) launched by the Danish Environmental Protection Agency.

We will describe the model construction step by step. First we will explain how the seabed is constructed within the model and how nutrient transport and processes are described. We will then discuss how values are assigned to the governing parameters and constants of the model and, finally, we will describe the running in, or adjustment, of the model before letting the whole thing loose on data from the HAV90 year.

2.1 Principles of the sediment flux model

The sediment flux model is a *time-dependent, one-dimensional transport-reaction model.* By including *time* as a variable we can describe the seasonal variation within the sediment and investigate the response time following one or more changes in environmental conditions. The model describes the seabed in *one dimension*: depth. Although variations in substance concentrations and process rates are in fact three-dimensional, the variation with depth is by far the greatest, and it is a fairly good approximation to consider this one dimension alone. Thus, the model results should be seen as averages for a relatively large area of seabed, 1 m^2 in size or more. Concentrations of the substances included in the model are affected at a given depth partly by *transport* to and from this depth and partly by *reaction*, i.e. consumption and/or production at that depth.

In the preceding chapter we saw that the carbon cycle can be divided into a series of sub-cycles that dominate organic matter degradation to varying degrees at different depths within the sediment. For instance, the nitrogen cycle is especially dominating in the upper few millimetres of the sediment below the oxidised zone (see Figure 1.6), while bacterial respiration with sulphate is more important deeper

down (see Figure 1.12). The relative depth distribution of the different processes is adjusted in a dynamic fashion depending on environmental conditions. It is impossible to determine beforehand where in the seabed the individual processes dominate and their quantitative importance to material cycling, or, for that matter, to sediment oxygen consumption. To achieve the highest possible degree of freedom and hence applicability for the sediment flux model we therefore assume that all processes (R1-R19, Chapter 1) can take place at all depths within the sediment. Whether or not a process does take place at a given depth, or rather, the rate at which it takes place, depends for instance on the concentrations of the chemical compounds entering into the process. This will be discussed in more detail later in this chapter.

We know empirically that by far the greater part of organic matter degradation influencing nutrient exchange between sediment and water column in Aarhus Bay takes place in the upper 20 cm of the seabed. This applies to most other coastal sediments as well. Therefore, we limit the scope of the sediment flux model to "merely" performing calculations concerning all significant sediment processes in the depth interval 0-20 cm. In other words, the challenge of constructing the model lies in converting the chemical reactions (R1-R19) into mathematical expressions and combining them with expressions of nutrient transport to enable us to carry out such calculations.

2.1.1 Stratification of the model

In order to describe mathematically the transport and nutrient cycling taking place in the depth interval 0-20 cm we perceive the seabed to be composed of numerous discs or layers. To be precise, the model consists of 105 layers including a 0.3-mm "water layer" overlying the sediment (Figure 2.1). This layer represents the very lowest part of the water column, which we call the diffusive boundary layer (DBL). The diffusive boundary layer differs from the rest of the water column in that transport of solutes takes place mainly by molecular diffusion. In principle, all chemical reactions can take place in each of the model's 105 layers. We know that the vast majority of the sediment processes take place in the uppermost few centimetres of the sediment, while the number of processes and the process rates both decrease with depth. We use this knowledge to obtain the largest possible resolution of the depth distribution of the processes. In other words, not all sediment layers in the model are of the same thickness. At the top of the model where many processes dominate separately in the uppermost few cm and conditions change rapidly with depth, the model is made up of many thin layers. Here, close to the sediment surface, the thickness of the layers is only 0.3 mm. Deeper down in the seabed, conditions change more slowly and, hence, the thickness of the layers may be up to 7 mm (Figure 2.1).

Bottom-water oxygen and nutrient concentrations are of great importance to the chemical processes in the sediment and to nutrient exchange between seabed and bottom water. Therefore, measured concentrations of O_2, NO_3^-, NH_4^+ and PO_4^{3+} are significant input parameters to the model. Exchange of these compounds between
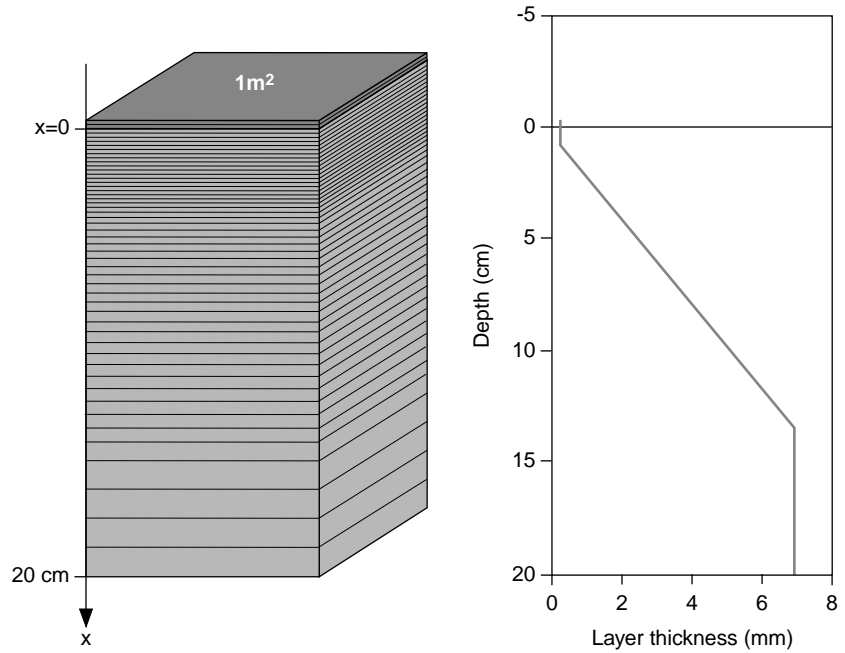
Figure 2.1. The mathematical sediment flux model, which calculates the cycling of nutrients in the seabed and the exchange of nutrients between sediment and bottom water, is divided into 105 layers. The top layer represents the very lowest part of the water column corresponding to the diffusive boundary layer (DBL), while the underlying layers represent the sediment. At the top, the layers are only 0.3 mm in thickness, but at a depth of 0.8 mm the thickness of the layers begins to increase linearly reaching 7 mm at a depth of 14 cm.

bottom water and sediment takes place via the diffusive boundary layer which is why it is included in the uppermost layer of the model.

In all of the 105 model layers a concentration is calculated at each time t for each of the model's 17 substances. The model operates by calculating new concentrations of all 17 substances each time the model moves one step forward in time ($t + \Delta t$). Each step represents 200 seconds. We will describe later how the model makes these calculations.

2.1.2   Material balance in the model layers

An element central to the model is the material balance in each of the model layers (Figure 2.2). In the model, concentrations of solutes are expressed in nmol cm^{-3} (pore water) and solids in nmol g^{-1} (dry weight). Thus, the balance in the layer j of the solute C is expressed as

$$\varphi_j \frac{\Delta C_j}{\Delta t} \Delta x_j = P_j$$

(Eq.1)

and, in the case of solids, by

$$\rho_s (1 - \varphi_j) \frac{\Delta C_j}{\Delta t} \Delta x_j = P_j$$

(Eq.2)
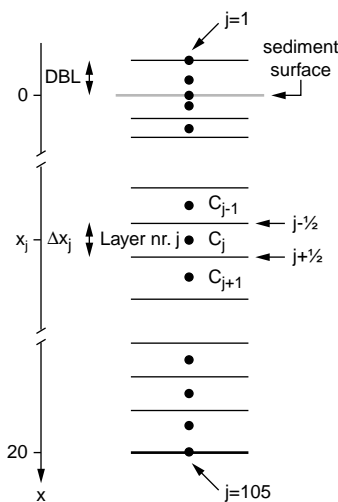
Figure 2.2. Overview of the sediment flux model nomenclature used in text and formulas.

31

where φ is porosity (i.e. sediment pore volume relative to total volume), ΔC_j the concentration change in the time interval Δt (200 seconds in the model), Δx_j the thickness of the layer, ρ_s the density of the solid sediment, and P_j the sum of material transport or material flux (negative or positive) across the upper and lower boundaries of the layer and net production/consumption of the material C in the layer. Thus, the equations express that the concentration change (ΔC) in the layer *j* during the time Δt equals the material flux to and from the layer plus the net material production in the layer. As we shall see later on, we use the equations to calculate new values of all concentrations at the time $t+\Delta t$ from known concentrations at the time *t*.

2.2   Material transport

Four different types of transport enter into the model, all describing vertical material transport in the seabed: molecular diffusion, bioturbation or biomixing, bioirrigation and sedimentation. Molecular diffusion applies only to solutes, while bioturbation affects both solutes and solids, when the animals responsible for this type of transport move around in and on the sediment. Bioirrigation applies only to solutes and is caused by tube-dwelling animals pumping water into and out of the seabed. Through sedimentation, material is deposited continuously on the seabed, and in this way both solutes and solids are constantly being buries in the sediment. To calculate the four types of material transport the model uses the commonly recognised mathematical expressions described in the following.

2.2.1   Molecular diffusion

The vertical flux of a solute transported by molecular diffusion is given by Fick's First Law

$$F_D = -\varphi D_s \frac{\Delta C}{\Delta x} \qquad \text{(Eq.3)}$$

where φ is porosity, D_s sediment diffusivity and $\Delta C/\Delta x$ the concentration gradient. D_s can be calculated by the following empirical expression: $D_s = \dfrac{D}{1+3(1-\varphi)}$ where *D* is the diffusivity of the material in pure seawater.

This expression takes into account that diffusion in sediment is slower because of the obstacles presented by sediment particles. Values of *D*, or rather, temperature-dependent values of *D*, can be found in the literature for all solutes included in the model, and apparently vary considerably within each separate material. For instance, in the case of O_2 *D* is doubled at a temperature increase of approximately $20^{\circ}C$. Thus, temperature significantly influences the amount of O_2 that is transported into the sediment at different times of the year, as annual bottom-water temperatures in Aarhus Bay vary up to $15^{\circ}C$.

The model uses Eq.3 to calculate fluxes taking place by molecular diffusion between layers. When we use the index *j-½* to refer to the upper boundary of layer *j* – i.e. the interface between layer j and layer *j-1* – the flux across this interface can be expressed as

$$F_{D\ j-\frac{1}{2}} = -\varphi_{j-\frac{1}{2}}D_{sj-\frac{1}{2}}\frac{C_j - C_{j-1}}{0,5(\Delta x_j + \Delta x_{j-1})}$$ (Eq.3$_{(j-\frac{1}{2})}$)

The flux across the lower interface of layer *j, j+½*, is calculated in the same way

$$F_{D\ j+\frac{1}{2}} = -\varphi_{j+\frac{1}{2}}D_{s\ j+\frac{1}{2}}\frac{C_{j+1} - C_j}{0,5(\Delta x_j + \Delta x_{j+1})}$$ (Eq.3$_{(j+\frac{1}{2})}$)

The fluxes $F_{D\ j-\frac{1}{2}}$ and $F_{D\ j+\frac{1}{2}}$ form part of the balance of layer *j* (equation Eq.1), so it follows that apart from the concentration of the substance *C* in layer *j* (C_j), the balance of layer *j* is dependent on the concentrations in the adjacent layers, C_{j-1} and C_{j+1}, respectively (Figure 2.2). Thus, the balances of the layers are linked, as they depend upon and influence each other. This linkage correctly expresses that the flux "running" from one layer across e.g. its lower boundary is identical to the flux "running" into the layer below, across its upper boundary.

2.2.2 Bioturbation and bioirrigation

Mathematically, the model represents the average of a relatively large area (1 m^2 or more; see Figure 2.1), which allowa us, with a good approximation, to describe bioturbation as a diffusive process even though mixing actually takes place as a series of local, discrete events. Thus, the flux of a solute by bioturbation may be expressed as

$$F_{B\ w} = -\varphi D_{B\ w}\frac{\Delta C}{\Delta x}$$ (Eq.4)

where φ is porosity, D_{Bw} the coefficient of biodiffusion and $\Delta C/\Delta x$ the concentration gradient. The size of D_{Bw} at a given sediment depth depends on the number and species of animals and, of course, on their activity. Hence, it is characteristic of D_{Bw} that it invariably decreases towards zero below a certain sediment depth. In recent years more attention has been directed towards the importance of bioturbation to sediment transport. It is not uncommon that bioturbation in the upper centimetres of the seabed is as significant as molecular diffusion. Recent research shows that the impact of bioturbation on solutes and solids, respectively, differs. Hence, it is not unusual for the coefficient of diffusion of a solute to be 10 times as large as that of a solid. Therefore, there is a sharp distinction between the coefficient of biodiffusion of solutes (D_{Bw}) and that of solids (D_{Bs}). On the other hand, the same coefficient is used for all solutes and all solids, respectively, as animals do not distinguish between different substances.

Thus, the flux of a solid by bioturbation may be expressed as

$$F_{Bs} = -\rho_s(1-\varphi)D_{Bs}\frac{\Delta C}{\Delta x}$$ (Eq.5)

where ρ_s is the density of the solid sediment. (Regarding the other symbols, please see Eq.4).

Material transport by irrigation can not be described as a diffusive transport in the same way as bioturbation. Instead, the model calculates the amount of material added to or removed from a sediment layer j in the concentration C_j by the following expression:

$$P_{Ij} = \varphi_j\alpha_j(C_0 - C_j)\Delta x_j$$ (Eq.6)

where φ_j is the layer's porosity, α_j the layer's irrigation parameter, C_0 the bottom-water concentration of the substance and Δx_j the thickness of the layer. The expression reflects that it is not a question of material transport taking place from an adjacent layer, but of the bottom water and the depth x_j being connected directly with each other. For that reason, P_{Ij} is also called a "non-local" transport contribution and this means that when C_0 is larger than C_j, i.e. if the bottom-water concentration is greater than that in the sediment, $P_{Ij} > 0$ and material is thus being added to the layer. Conversely, when C_0 is smaller than C_j material is being removed from the layer.

In reality, biorrigation is a much more complex and multidimensional phenomenon than described in this presentation, and equation Eq.6 may therefore seem overly simplified and stylised. Thus, we must keep in mind that when bioirrigation contributes significantly to transport, the bottom-dwelling animals responsible are often many and divers. This means that a simple model description of bioirrigation can only be achieved because the model represents an average covering a relatively large area (1 m² or more).

The size of the irrigation parameter α at a given sediment depth depends on the number, species and activity of animals. Hence, it is characteristic of α that it invariably decreases towards zero below a certain sediment depth.

Irrigation is the quickest way for solutes to be transported between sediment and bottom water because the substances take a shortcut, so to speak, through the tubes or small channels in which the irrigating animals live. Thus, solutes are able to quickly leave or enter the sediment. By molecular diffusion and bioturbation substances must pass through all sediment layers, which, of course, is slower than material transport by irrigation. Both bioirrigation and bioturbation are limited to the uppermost, fauna-inhabited sediment layers, however, whereas molecular diffusion takes place anywhere in the sediment where a concentration gradient of a given substance is found.

2.2.2.1 Bioactivity

Bioturbation and bioirrigation enter into the sediment flux model as transport mechanisms resulting from the presence of animals in or on the sediment.

Several of the scenarios that were to be calculated for Aarhus Bay represent periods in which little or no oxygen is present in the bottom-water. It is a well-known fact that poor bottom-water oxygen conditions have a significant impact on the (bio)activity of bottom-dwelling animals. Therefore, we have chosen to correct the sediment flux model for animal activity in cases of bottom-water oxygen depletion. To put it differently, we have set up a number of mathematical expressions describing theoretically how we believe bioturbation and bioirrigation are reduced during and after the occurrence of bottom-water oxygen depletion.

When the sediment flux model was set up for the HAV90 year, bottom-water oxygen depletion did not occur at any point. In other words, transport coefficients were determined for both bioturbation and bioirrigation without sediment animal activity being affected by low oxygen levels. Hence, it seems natural to let these transport coefficients represent a situation in which both the number and distribution of animals are at a "natural" or "normal" level.

We therefore introduce into the sediment flux model an index (A) of bioactivity correcting for animal bioturbation and bioirrigation relative to the HAV90 year. The index A may assume all values between 1 and 0. If A equals 1, animal activity is the same as in the HAV90 year. Conversely, bioactivity is 0 if all animals are inactive and all transport taking place by bioturbation or bioirrigation has ceased. The model adjusts bioturbation and bioirrigation values by multiplying the transport coefficients calculated in the run-in phase of the model by A. It follows that when bioactivity is adjusted in this way, the model is unable to increase bioturbation or bioirrigation intensities beyond the levels found in the HAV90 year. In other words, bioactivity was at its maximum in the HAV90 year.

The index A changes during the time ($\Delta A/\Delta t$) in the following way

$$\frac{\Delta A}{\Delta t} = -K_m \, A + K_v \, (1 - A) \qquad \text{(Eq.7)}$$

where K_m and K_v are potential rates expressing how quickly animals are inactivated (die) under poor oxygen conditions and activated (grow) when oxygen conditions improve, respectively. Both K_m and K_v are dependent on the prevailing conditions, as described below. Note that if A is 0 all animals are inactive or dead and the value of K_m is consequently insignificant. Similarly, K_v is of no significance to the activation or growth of animals if bioactivity (A) is 1 already. As we shall see later on in this chapter (regarding the other variables of the model), A, too, may be projected from the time t to $t + \Delta t$ if the values A at the time t and $\Delta A/\Delta t$ are known.

The potential rate K_m is dependent on the bottom-water oxygen concentration and is calculated by the following set of equations

$$\begin{cases} K_m = 0\,\mathrm{d}^{-1} & \text{for } [O_2] > 2\,\mathrm{mg}\,O_2\,\mathrm{liter}^{-1} \\ K_m = 0{,}2\,e^{(-[O_2]/0{,}382)}\,\mathrm{d}^{-1} & \text{for } [O_2] \leq 2\,\mathrm{mg}\,O_2\,\mathrm{liter}^{-1} \end{cases} \qquad \text{(Eq. 8)}$$

In the model the value of the rate K_m is defined so as to reflect no inactivation of animals ($K_m = 0$ d^{-1}) when $[O_2] > 2$ mg O_2 liter^{-1}. In cases of severe bottom-water oxygen depletion, i.e. when $[O_2] \leq 2$ mg O_2 liter^{-1}, inactivation of animals in and on the seabed increases exponentially, and K_m approaches its maximum (0,2 d^{-1}) as all oxygen disappears from the bottom water (Figure 2.3).
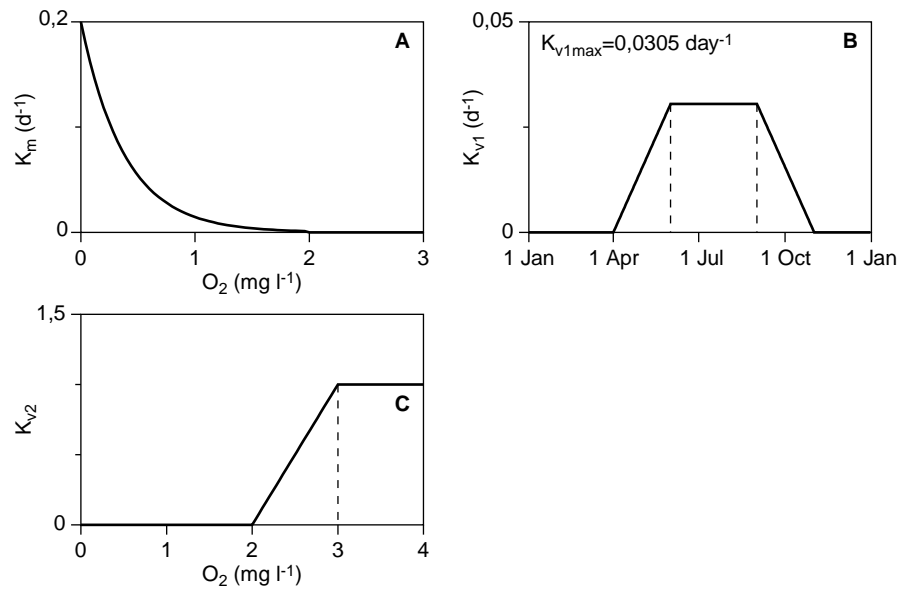
Figure 2.3. K_m and K_v are potential rates expressing how quickly animals are inactivated (die) under poor oxygen conditions and activated (grow) when oxygen conditions improve, respectively. The variation in K_v is composed of two variables K_{v1} and K_{v2} (see text) A: The variation in K_m as a function of the O_2 concentration shows that, in the model, bottom-dwelling animals are inactivated at O_2 concentrations < 2 mg O_2 liter^{-1}. B: K_{v1} as a function of the time of year shows that, in the model, the growth season of bottom-dwelling animals is defined as 1 April to 31 October. C: K_{v2} as a function of the O_2 concentration shows that the model requires > 2 mg O_2 liter^{-1} for activation of benthic animals to take place.

The rate K_v, which expresses how quickly animals are activated (grow) when bottom-water oxygen conditions improve, is dependent on both time of year and prevailing oxygen conditions. Therefore, K_v is composed of the two variables

$$K_v = K_{v1}\,K_{v2} \qquad \text{(Eq. 9)}$$

where K_{v1} is the potential rate of animal activation depending on time of year, and K_{v2} expresses that a bottom-water O_2 concentration of more than 2 mg O_2 liter^{-1} is required for animals to be activated.

In the sediment flux model K_{v1} is chosen so that potential activation of animals increases linearly from 0 d^{-1} (31 March) and reaches the maximum value (0,0305 d^{-1}) at which it remains from 1 June to 31 August (Figure 2.3B). K_{v1} then decreases linearly from 1 September to 31 October. During the months November-March $K_{v1} = 0$ d^{-1}. In other words, animals can only be activated in the period April-October, if oxygen conditions are sufficiently favourable, and only until bioactivity reaches the value 1.

We have constructed K_{v2} so as to ensure that it assumes a value of 0 at oxygen concentrations ≤ 2 mg O_2 liter^{-1} and increases linearly to 1 when the oxygen concentration increases from 2 to 3 mg O_2 liter^{-1} (Figure 2.3C). In other words, animals are able to achieve their maximum growth rates in the summer months of June, July and August, only if oxygen conditions allow it, i.e. if $[O_2] \geq 3$ mg O_2 liter^{-1}.

In Figure 2.4 two examples are given of variations in sediment bioactivity resulting from variations in bottom-water oxygen conditions. The figure illustrates clearly that worsening bottom-water oxygen conditions lead to rapid inactivation (death) of benthic animals (Figure 2.4A). Similarly, it is evident that benthic animals are not activated until spring (Figure 2.4B), i.e. not until 1 April, for instance through recolonisation of the seabed, and that maximum growth rates are not achieved until oxygen concentrations exceed 3 mg O_2 liter^{-1}.
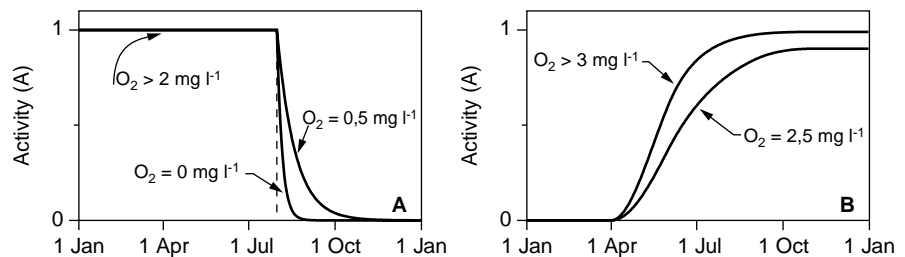
Figure 2.4. A: Examples of inactivation of benthic animals in connection with sudden oxygen depletion (0.5 and 0 mg O_2 liter^{-1}, respectively). B: Examples of animal activation/recolonisation when oxygen conditions improve (2.5 and 3 mg O_2 liter^{-1}, respectively).

2.2.3 Burial of dissolved and solid substances

A vast majority of marine localities are subject to net deposition of sediment particles with time. In other words, relative to an absolute fixed point the seabed grows. In the model this reference point (x=0) is placed by definition at the sediment surface (Figure 2.2), and all sedimentation thus corresponds to a downward transport away from the surface. Both dissolved and solid substances are buried in the seabed as sediment moves downwards through the layers, so to speak, and ends up "dropping out" of the bottom of the model at a depth of 20 cm.

The burial flux of solutes (F_{Cw}) can be calculated as

$$F_{Cw} = \varphi u C \qquad \text{(Eq.10)}$$

and, in the case of solids, by

$$F_{Cs} = \rho_s (1 - \varphi) w C \qquad \text{(Eq.11)}$$

where u and w are the burial rates of solutes and solids, respectively. Below the depth where the sediment is compressed no further (i.e. the depth below which φ is constant) u and w are identical. The burial flux is generally insignificant in regard to solutes, while constituting the only transport form for solids in depths where bioturbation is no longer significant.

2.2.4 Adsorption

Some of the solutes entering into the model (NH_4^+, Mn^{2+}, Fe^{2+} and PO_4^{3-}) may to a greater or lesser extent adsorb (i.e. bind) to solid sediment particles. Substantial adsorption of a substance may thus prove significant to transport of that substance, because the "normally" dissolved substance is now also being transported as if it were a solid.

Adsorption is included in the model under the assumption that all adsorption is reversible and in equilibrium with the surrounding pore water. Thus, the concentration of the adsorbed substance can be written, at all sediment depths, as

$$C_{ads} = K'C \qquad \text{(Eq.12)}$$

where K' is the adsorption coefficient and C the total pore-water concentration of the substance. Hence, the total flux, resulting from bioturbation for instance, of a dissolved substance that also adsorbs to sediment particles becomes:

$$F_{Bw} = -\varphi D_{Bw} \frac{\Delta C}{\Delta x} - \rho_s (1 - \varphi) D_{Bs} \frac{K'\Delta C}{\Delta x} \qquad \text{(Eq.13)}$$

where the first term is identical to Eq.4 (bioturbation of solutes) and the second term covers the adsorbed portion of the substance, which behaves like a solid. Thus, the second term also corresponds to the expression in Eq.5.

2.3 The general mass balance

The contributions or equations described in the above (Eq.3-Eq.6 and Eq.10-Eq.13) representing the various types of transport can now be substituted into Eq.1 and Eq.2, respectively. This provides us with the two new mass balance expressions constituting the corner stones of the model. If we combine the two equations and write the result in differential form, we arrive at the following general equation

$$\left(\xi\varphi + \rho_s\left(1-\varphi\right)K'\right)\frac{\partial C}{\partial t} = \frac{\partial}{\partial x}\left(\left(\xi\varphi\left(D_{Bw} + D_s\right) + \rho_s\left(1-\varphi\right)D_{Bs}K'\right)\frac{\partial C}{\partial x}\right) -$$

$$\frac{\partial}{\partial x}\left(\left(\xi\left(\varphi u\right)_x + \rho_s\left(\left(1-\varphi\right)w\right)_x K'\right)C\right) + \xi\varphi\alpha\left(C_0 - C\right) + R \qquad \text{(Eq.14)}$$

where R is net production, which is negative in the event of net consumption of the substance. The parameter ξ is of no consequence biologically, but constitutes an auxiliary variable assuming the value 1 when the substance is a solute and 0 when the substance is a solid. For explanations of the remaining symbols, please refer to those given in connection with Eq.1-Eq.6 and Eq.10-Eq.13.

As described in the following, equation Eq.14 is solved for each substance entering into the model, for each of the model's 105 layers and for each time step. Before we can achieve this, however, we must determine the production and consumption of the various substances or, in other words, get a grip on the variable R.

2.4 Production and consumption of substances in the model

Unlike the types of transport entering into the model (molecular diffusion, bioturbation, bioirrigation and burial) production and consumption are dependent only on substance concentrations in the relevant depths, i.e. the layers where the reactions take place. The relation between production and consumption is reflected in the stoichiometry of the various chemical reactions in which the substances are involved (Table 2.1). Thus, all that remains is to quantify the individual reaction rates, and we will have sufficient information to solve Eq.14.

Many previous model studies have forcibly regulated the various chemical reactions by allowing them to take place only in well-defined depth intervals. In this way the flexibility of the model becomes strongly limited, ruling out general application. In the sediment flux model described here, regulation of individual reactions is expressed solely by the substance concentrations in each of the 105 model layers. Thus, the various substances can be produced or consumed freely at all depths so that the balance between production, consumption, transport to and from layers and substance concentrations in the separate layers is preserved.

Table 2.1. Chemical reactions entering into the sediment flux model (see Figure 1.13).

Primary reactions

$O_2 + CH_2O \rightarrow CO_2 + H_2O$	(R1)
$4NO_3^- + 5CH_2O + 4H^+ \rightarrow N_2 + 5CO_2 + 7H_2O$	(R2)
$2MnO_2 + CH_2O + 4H^+ \rightarrow 2Mn^{2+} + CO_2 + 3H_2O$	(R3)
$4FeOOH + CH_2O + 8H^+ \rightarrow 4Fe^{2+} + CO_2 + 7H_2O$	(R4)
$SO_4^{2-} + 2CH_2O + 2H^+ \rightarrow H_2S + 2CO_2 + 2H_2O$	(R5)

Secondary reactions

$NH_4^+ + 2O_2 \rightarrow NO_3^- + H_2O + 2H^+$	(R6)
$FeOOH + PO_4^{3-} \rightarrow FeOOH \equiv PO_4^{3-}$	(R7)
$2Fe^{2+} + MnO_2 + 2H_2O \rightarrow 2FeOOH + Mn^{2+} + 2H^+$	(R8)
$2Mn^{2+} + O_2 + 2H_2O \rightarrow 2MnO_2 + 4H^+$	(R9)
$H_2S + 2FeOOH \equiv PO_4^{3-} + 4H^+ \rightarrow S^o + 2Fe^{2+} + 4H_2O + 2PO_4^{3-}$	(R10a)
$4Fe^{2+} + O_2 + 6H_2O \rightarrow 4FeOOH + 8H^+$	(R11)
$H_2S + 2FeOOH + 4H^+ \rightarrow S^o + 2Fe^{2+} + 4H_2O$	(R10b)
$H_2S + MnO_2 + 2H^+ \rightarrow S^o + Mn^{2+} + 2H_2O$	(R12)
$H_2S + Fe^{2+} \rightarrow FeS + 2H^+$	(R13)
$FeS + S^o \rightarrow FeS_2$	(R14)
$SO_4^{2-} + 3H_2S + 4FeS + 2H^+ \rightarrow 4FeS_2 + 4H_2O$	(R15)
$H_2S + 2O_2 \rightarrow SO_4^{2-} + 2H^+$	(R16)
$FeS + 2O_2 \rightarrow Fe^{2+} + SO_4^{2-}$	(R17)
$2FeS_2 + 7O_2 + 2H_2O \rightarrow 2Fe^{2+} + 4SO_4^{2-} + 4H^+$	(R18)
$4S^o + 4H_2O \rightarrow 3H_2S + SO_4^{2-} + 2H^+$	(R19)

2.4.1 Primary reactions

The degradation of organic material takes place through the primary reactions (R1-R5; Table 2.1 and Figure 1.2). Numerous studies have shown that organic material deposited on marine sediments can be divided into different pools:

- a pool that is degraded rapidly (CH_2O_f) i.e. within few weeks or months – the index f denotes "fast"

- a pool that is degraded significantly more slowly (CH_2O_s) typically over several years – the index s denotes "slow"

- a pool that is not degraded at all (CH_2O_n) – the index n denotes "non"

These studies give an indication of the relative distribution of the three pools and the degradation rates of the two degradable pools.

As an example of organic matter degradation we will look at the way in which the degradation of CH_2O_s is regulated. First, the total

degradation of the slowly degradable pool is calculated and then it is distributed among the five primary reactions (R1-R5).

Total degradation (V_s) can be calculated by

$$V_s = K_{\mathrm{OM}\,s}(1-\varphi)\rho_s[\mathrm{CH_2O}_s] \qquad\qquad (\text{Eq.15})$$

where $K_{\mathrm{OM}\,s}$ is the rate constant of the $\mathrm{CH_2O}_s$ pool. The two factors *(1 – φ)* and ρ_s are simply conversion factors giving V_s the same unit as R in Eq.14, i.e. nmol s^{-1} cm^{-3} (sediment). Put into words, Eq.15 expresses that degradation of the slowly degradable pool of organic matter is proportional to the amount. This corresponds well with *in situ* observations showing that bacterial degradation rates are almost always limited by the amount of organic matter. As [$\mathrm{CH_2O}_s$] generally decreases with depth and V_s is calculated for each layer in the sediment flux model, V_s, too, tends to decrease with depth. After calculation of V_s (and of V_f for that matter) it remains only to distribute the degradation of organic matter among the five primary reactions.

The five primary reactions, R1-R5, are numbered in an order reflecting the energy obtained by the bacteria by degrading organic matter using oxygen, nitrate, manganese, iron and sulphate, respectively. Degradation with oxygen (R1) is the most energy-yielding process, while sulphate reduction (R5) is the respiration process yielding least energy. In the seabed these oxidants are consumed in exactly that order, which explains the characteristic appearance of the concentration profiles of O_2, NO_3^-, MnO_2, FeOOH and SO_4^{2-} within the sediment (Figure 1.2).

Many studies have shown that the different respiration processes form a successive pattern down through the sediment. In other words, the denitrification process (R2) does not begin until almost all O_2 is consumed by the process R1, that manganese respiration (R3) begins only when almost all NO_3^- is gone etc. Competition between the different groups of bacteria responsible for degradation is the factor controlling this hierarchy. In the model the hierarchy is reflected in the distribution of V_s among the five primary reactions. Provided oxygen is present in the bottom water and hence in the uppermost sediment layer, V_{s1} (the process rate of $\mathrm{CH_2O}_s$ degradation via R1) equals V_s until the depth where the oxygen concentration has decreased to a certain value, $O_{2\text{ lim}}$. At this depth the contribution of denitrification (R2) to degradation gradually begins to increase, but the process does not reach its maximum until all oxygen is consumed. Deeper in the sediment manganese oxidation (R3) begins to increase, coincident with a decrease in the NO_3^- concentration to the value $NO_{3\text{ lim}}^-$ and so forth. Thus, with respect to R1 and R2, regulation can be expressed mathematically by the following equation

$$\left\{\begin{array}{l} [O_2] > [O_{2\lim}]: \quad V_{s1} = V_s \qquad\qquad \text{og} \qquad V_{s2} = 0 \\[3mm] [O_2] \le [O_{2\lim}]: \quad V_{s1} = V_s \dfrac{[O_2]}{[O_{2\lim}]} \quad \text{og} \quad V_{s2} = V_s\left(1 - \dfrac{[O_2]}{[O_{2\lim}]}\right) \end{array}\right\} \quad \text{(Eq.16)}$$

Equivalent expressions can be formulated for V_{s3}, V_{s4} and V_{s5}. It is evident that at all depths $V_s = V_{s1} + V_{s2} + V_{s3} + V_{s4} + V_{s5}$. Only four so-called limiting concentrations are needed as input to the model: $O_{2\lim}$, $NO_{3\lim}^-$, $MnO_{2\lim}$ and $FeOOH_{\lim}$, as no limiting concentration of SO_4^{2-} is applied. We assume that sufficient SO_4^{2-} is always present in the sediment for this process to take place without the SO_4^{2-} concentration limiting degradation. This assumption is definitely valid for Aarhus Bay according to measurements in the uppermost 20 cm of the seabed covered by the model.

The degradation of the readily degradable pool (CH_2O_f) is determined in the exact same way, except that the rate constant $K_{OM\,f}$ is considerably greater.

Degradation of the two organic matter pools is therefore regulated only by the organic matter concentrations calculated by the model. In the individual layers the processes (R1-R5) are thus free to adjust to the prevailing conditions, such as oxygen conditions in the bottom-water and uppermost in the sediment. In some zones, which may consist of one or more layers, some processes will decrease, therefore, while others increase.

2.4.2 Secondary reactions

The rate at which the secondary reactions (R6-R19) take place is governed by the concentrations of the substances involved in the chemical reaction in question. To illustrate this, we will take a look at the process rate of R16 (i.e. $H_2S + 2O_2 \rightarrow SO_4^{2-} + 2H^+$)

$$V_{16} = K_{16}\varphi[H_2S][O_2] \qquad\qquad \text{(Eq.17)}$$

where *[H$_2$S]* and *[O$_2$]* are the concentrations of the two reactants in R16 and K_{16} the rate constant of the process. Porosity, φ, enters into the equation as a conversion factor giving V_{16} the same unit (nmol s^{-1} cm^{-3}) as R in equation Eq. 14. Among other things, regulation expresses that if the concentration of one reactant reaches zero at a certain depth, the process stops. Conversely, the process rate is doubled if the concentration of one of the reactants is doubled. Like all other process rates, the process rate V_{16} is calculated for each layer.

Two chemical substances in the sediment need special mention. These are oxidised iron and oxidised manganese, both of which are solids. What makes FeOOH and MnO_2 special is the fact that these compounds grow more stable with age. In other words, while the degradation of oxidised iron and manganese is rapid at first, it becomes increasingly slow with time and the compounds end up in a crystalline and virtually undegradable state. In the model we are content with dividing FeOOH and MnO_2 into a degradable pool

(FeOOH$_A$ and MnO$_{2A}$, respectively) and an undegradable pool (FeOOH$_B$ and MnO$_{2B}$, respectively). The chemical equations of the conversion of degradable to undegradable material becomes

$$MnO_{2A} \rightarrow MnO_{2B} \tag{R20}$$
$$FeOOH_A \rightarrow FeOOH_B \tag{R21}$$

For example, the degradation rate of MnO$_{2A}$ to MnO$_{2B}$ can be calculated as

$$V_{20} = K_{20}(1-\varphi)\rho_s[MnO_{2A}] \tag{Eq.18}$$

where *(1-φ)* and ρ_s are conversion factors giving V_{20} the same unit as *R* in equation Eq.14. The same regulation applies in the degradation of FeOOH$_A$ to FeOOH$_B$ (R21).

An example of a process that is inhibited by its own product is the disproportionation of particulate sulphur (R19). Disproportionation yields both H$_2$S and SO$_4^{2-}$ but only as long as the concentration of H$_2$S remains below a certain limit (H$_2$S$_{stop}$). Therefore, the reaction rate of this process is calculated in two steps. First, the process rate without inhibition is calculated

$$\tilde{V}_{19} = K_{19}(1-\varphi)\rho_s[S^0] \tag{Eq.19}$$

after which $\tilde{V}_{19}$ is reduced depending on the prevailing H$_2$S concentration

$$\left\{ \begin{array}{ll} [H_2S] < [H_2S]_{stop}: & V_{19} = \tilde{V}_{19}\left(1 - \dfrac{[H_2S]}{[H_2S]_{stop}}\right) \\[4mm] [H_2S] \geq [H_2S]_{stop}: & V_{19} = 0 \end{array} \right\} \tag{Eq.20}$$

where *[H$_2$S]$_{stop}$* is the H$_2$S concentration at which the process is 100% inhibited. This regulation also expresses that the process is not inhibited at all when the H$_2$S concentration is zero.

2.5   Temperature dependency

The rates of the primary and secondary reactions depend also on the temperature in the seabed. In the case of the majority of the reactions, present knowledge of their temperature dependency is far from complete. Several process studies have shown, however, that primary reactions tend to be more dependent on temperature than secondary reactions. Therefore, we have chosen to introduce two different temperature regulation mechanisms in the model; one for primary reactions and one for secondary reactions. Both regulation mechanisms are based on the well-known regulation factor Q_{10}, i.e. the factor by which process rates increase at a temperature increase of 10^oC, all other parameters being constant. The two Q_{10} values for

primary and secondary reactions, respectively, are used together with rate constants and the various transport parameters as input to the model. Later on in this chapter we will describe how these values are determined.

2.6 Boundary conditions

We described above how the material balances of the model layers are linked. For instance, apart from the concentration in the layer itself, the material balance in layer *j* depends on concentrations in the two adjacent layers *j-1* and *j+1*, i.e. the ones above and below the layer *j*, respectively, (Figure 2,2). Similarly, the uppermost layer of the model, corresponding to the diffusive boundary layer, is linked to a non-existent layer above it, just as the lowermost layer at a depth of 20 cm is linked to a non-existent layer below it. Therefore, the model requires that a so-called boundary condition be specified at the top of the uppermost layer and at the bottom of the lowermost layer, respectively, for each substance entering into the model calculations

The boundary conditions, which in a dynamic calculation may vary temporally, may assume three different forms:
1. a known concentration
2. a known flux
3. a known concentration gradient

At first sight, these boundary conditions may seem difficult to specify, but that is far from the case. At the bottom of the model virtually all reactions (R1-R19) have stopped and, therefore, all concentration gradients are close to being zero (boundary condition 3). For several solid substances a corresponding "zero flux" can be specified for the uppermost layer of the model (boundary condition 2). Bottom-water concentrations of dissolved substances are measured routinely and may therefore be used as boundary condition for the uppermost model layer (boundary condition 1). Finally, there is the addition of organic material to the uppermost layer of the model. This is one of the most important input parameters to the sediment flux model, and naturally has a known flux specified to it (boundary condition 2).

The two solids MnO_2 and FeOOH have special boundary conditions. An undefined portion of Mn^{2+} and Fe^{2+} will, primarily by irrigation, be transported from the sediment to the bottom water Here, the substances react immediately with O_2 to form MnO_2 and FeOOH, respectively, which then fall to the sediment surface. In other words, when the model calculates the flux of Mn^{2+} and Fe^{2+} from the seabed to the bottom water, this flux equilibrates with a corresponding downward flux of MnO_2 and FeOOH. To this must be added external flux contributions of MnO_2 and FeOOH. External contributions are necessary, so to speak, because both manganese and iron are continuously disappearing through the bottom of the model via permanent burial. Thus, a known flux of Mn and Fe takes place from the bottom layer of the model (boundary condition 2), which gradually empties the sediment of iron and manganese if this loss is not covered by addition of MnO_2 and FeOOH to the top layer of the model.

2.7   The calculation flow of the model

In all 105 layers the model calculates the concentrations of the substances entering into the model as well as the fluxes of substances between layers. Of special interest in this context is the nutrient flux between the two model layers that have their boundaries at the sediment surface, i.e. the diffusive boundary layer and the uppermost sediment layer (Figure 2.2). It is the flux between these layers that expresses the nutrient exchange between bottom water and seabed.

A model simulation is divided temporally into many time steps ranging in length from a few minutes to one hour. The model calculates concentrations and fluxes of all substances between the layers in every single time step, and since a typical model simulation covers several years, sometimes even hundreds of years, the number of numerical calculation operations becomes very, very large, typically several millions of calculations. This is why the calculation algorithms that are executed in each time step are optimised with respect to calculation speed and, consequently, highly complex. The calculation flow can be explained, somewhat simplistically, in the following way:

Let us assume that the model is performing a model simulation and that the model in this series of calculation has reached the time t. At this point in time all substance concentrations in all 105 layers have just been calculated and are therefore known to the model. The model operates with time steps of Δt and must now in each layer project the concentration, production and consumption as well as the flux of substances between the layers to the time $t + \Delta t$.

First, the model calculates the rates of all processes (R1-R19) in all model layers at the time t. To make these calculations the model uses the known substance concentration at time t, the sediment temperature and, of course, the rate expressions Eq.15-Eq.20. The model then calculates the net production or consumption of each substance in the layers using knowledge of process rates and reaction stoichiometry. In the same way, the fluxes of all substances across the layer boundaries are calculated by using the expressions Eq.3-Eq.6, Eq.10-Eq.11 and Eq.13.

The model now assumes that all net production and flux values calculated at time t apply for the entire time step – i.e. from time t to time $t + \Delta t$. Thus, the model can calculate the material transport (P_j) to or from each layer at the time $t + \Delta t$, and by using equation Eq.1 or Eq.2 finally determine $\Delta C_j/\Delta t$. The model already knows the concentrations of all substances in all layers at time t, and can now easily calculate the new concentrations at time $t + \Delta t$. The calculation procedure is then repeated in a new time step, in which the model uses the approach described above to calculate new concentrations, fluxes etc. at time $t + 2\Delta t$.

Thus, the model calculates all concentrations, net productions and fluxes on the basis of information that, strictly speaking, only applies at time t. It is obvious that the larger the time steps used, the less

valid this approximation becomes. Therefore, the length of time steps used in model calculations is subject to strict regulation.

2.8   Input to the model

In this section we will describe how we determine the many constants and other input parameters that are more or less unique to the sediment being modelled. Obviously, describing how we arrive at each and every input parameter entering into the model would be too much. We will therefore limit the description to a few examples and, in addition, present an overview of all input parameters to the sediment flux model in Table 2.2.

Table 2.2. Input to the sediment flux model.

Parameter	Expression or value
Porosity	$\varphi = 0.763 + 0.086\, e^{-0.216x}$
Density	ρ_s = 2.04 g cm^{-3}
Diffusivity i free water[1]	D_{O2} = (11.7+0.344T+0.00505T^2) 10^{-6} cm^2 s^{-1}
	D_{NO3} = (9.72+0.365T) 10^{-6} cm^2 s^{-1}
	D_{N2} = (9.52+0.291T+0.00448T^2) 10^{-6} cm^2 s^{-1}
	D_{CO2} = (9.39+0.267T+0.0041T^2) 10^{-6} cm^2 s^{-1}
	D_{H2S} = (8.74+0.264T+0.004T^2) 10^{-6} cm^2 s^{-1}
	D_{SO4} = (4.96+0.226T) 10^{-6} cm^2 s^{-1}
	D_{NH4} = (9.76+0.398T) 10^{-6} cm^2 s^{-1}
	D_{Mn} = (3.04+0.153T) 10^{-6} cm^2 s^{-1}
	D_{Fe} = (3.36+0.148T) 10^{-6} cm^2 s^{-1}
Q$_{10}$ of primary processes	Q$_{10}$ = 3.8
Q$_{10}$ of secondary processes	Q$_{10}$ = 2.0
Biodiffusivity of solutes	$x \le$ 11.8 cm: D_{Bw} = 3.51 10^{-6} cm^2 s^{-1}
	x >11.8 cm: D_{Bw} = 3.51 10$^{-6}\, e^{-0.378(x-11.8)}$ cm^2 s^{-1}
Biodiffusivity of solids	$D_{Bs} = D_B$ / 9.3 cm^2 s^{-1}
Sedimentation rate	w = 0.064 cm $^{year-1}$
Bioirrigation parameter	α = 10$^{(0.885-0.054x+2.53*exp(-0.352x)}$ year^{-1}

Adsorption constants	$K'_{NH4} = 2.2 \ cm^3 \ g^{-1}$
	$K'_{Mn} = 13 \ cm^3 \ g^{-1}$
	$K'_{Fe} = 500 \ cm^3 \ g^{-1}$
	$K'_{PO4} = 2.0 \ cm^3 \ g^{-1}$
Diffusive boundary layer	$DBL = 0.03 \ cm$
External fluxes	$F_{MnO2} = 3.5 \ 10^{-6} \ nmol \ cm^{-2} \ s^{-1}$
	$F_{FeOOH} = 2.05 \ 10^{-4} \ nmol \ cm^{-2} \ s^{-1}$
Ratios	$F_{OM \ n}/F_{OM \ total} = 0.08$ (see text 5.1)
	$F_{OM \ f}/F_{OM \ total} = 0.42$
	$C:N = 10.0$
	$C:P = 80.0$
Limiting concentrations	$O_{2 \ lim} = 20 \ \mu M$
	$NO_{3 \ lim}^- = 5 \ \mu M$
	$MnO_{2 \ lim} = 50000 \ nmol \ g^{-1}$
	$FeOOH_{lim} = 100000 \ nmol \ g^{-1}$
Rate constants	$K_{OM \ f} = 9.6 \ 10^{-6} \ s^{-1}$
	$K_{OM \ s} = 1.2 \ 10^{-8} \ s^{-1}$
	$K_6 = 2.5 \ 10^{-6} \ \mu M^{-1} \ s^{-1}$
	$K_7 = 5.0 \ 10^{-11} \ s^{-1}$
	$K_8 = 1.7 \ 10^{-8} \ \mu M^{-1} \ s^{-1}$
	$K_9 = 1.5 \ 10^{-5} \ \mu M^{-1} \ s^{-1}$
	$K_{10} = 2.0 \ 10^{-8} \ \mu M^{-1} \ s^{-1}$
	$K_{11} = 5.0 \ 10^{-4} \ \mu M^{-1} \ s^{-1}$
	$K_{12} = 3.0 \ 10^{-9} \ \mu M^{-1} \ s^{-1}$
	$K_{13} = 7.5 \ 10^{-7} \ \mu M^{-1} \ s^{-1}$
	$K_{14} = 3.0 \ 10^{-12} \ cm^3 \ nmol^{-1} \ s^{-1}$
	$K_{15} = 2.5 \ 10^{-11} \ s^{-1}$
	$K_{16} = 5.0 \ 10^{-5} \ \mu M^{-1} \ s^{-1}$
	$K_{17} = 6.0 \ 10^{-7} \ \mu M^{-1} \ s^{-1}$
	$K_{18} = 1.6 \ 10^{-8} \ \mu M^{-1} \ s^{-1}$
	$K_{19} = 7.0 \ 10^{-7} \ s^{-1}$
	$K_{20} = 1.3 \ 10^{-9} \ s^{-1}$
	$K_{21} = 9.0 \ 10^{-10} \ s^{-1}$
Inhibiting concentration	$H_2S_{stop} = 10 \ \mu M$

1) T is the temperature in Celcius (°C)

Almost all constants are calculated on the basis of the very intensive measurements performed during the Marine Research Programme 1990. It is necessary, however, to assign values to certain constants before running the model in for the first time. Among others, this applies to the constant pertaining to sediment porosity and density. Other constants are found through trial and error, meaning that a
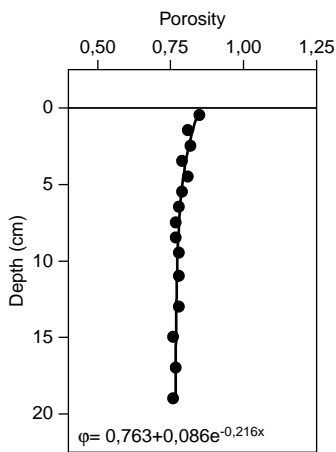
Figure 2.5. Porosity (φ) measured in the sediment of Aarhus Bay and approximated by an exponentially decreasing function.

$$\varphi = 0{,}763 + 0{,}086e^{-0{,}216x}$$

guess is made of the constant's value, after which the model is launched and the constant adjusted on the basis of comparison between results calculated by the model and the values measured. Among others, the rate constants of the reactions are found in this way.

2.8.1 Input determined before the model is run in

2.8.1.1 Porosity

A porosity (φ) is assigned to each model layer. Therefore, the porosity measured in the sediment is approximated by an exponentially decreasing function. The exponential function is then used to calculate porosity in each model layer (Figure 2.5, Table 2.2).

2.8.1.2 Density

Likewise, the density of the solid components of the sediment (ρ_s) is calculated from sediment measurements. This value is not affected by variations in porosity, which is why density only rarely varies with depth.

2.8.1.3 Diffusivity

Diffusivities of free-water solutes are temperature dependent. Thus, good descriptions of diffusivity can be obtained by adjusting values found in the literature using either a second order polynomial or a straight line. The temperature dependency of diffusivity is shown in Table 2.2.

2.8.1.4 Q_{10} value

The Q_{10} value determined for the primary reactions is based on sulphate reduction rates measured in Aarhus Bay. Apart from temperature, sulphate reduction in the upper seabed is influenced by the load of organic matter and the freshness of that matter. Therefore, only sulphate reduction rates in the depth interval 7-10 cm were used to determine the Q_{10} value. As shown in Figure 2,6 the rates are clearly correlated with temperature and by fitting the measured values we arrive at a Q_{10} value of 3.8, which we then use for all primary reactions. For the secondary reactions we use an estimated Q_{10} value of 2 based on values found in the literature.

2.8.1.5 Biodiffusivity

The biodiffusivity of solids (Eq.5) is found by interpretation of ^{210}Pb profiles from Aarhus Bay, concentration profiles and data on organic matter consumption. These interpretations show that biodiffusivity is more or less constant in the upper 12 cm, approximately, of the seabed, below which it decreases exponentially. Comparison of measured profiles and flux in the seabed shows that the biodiffusivity of solutes ($D_{B\,w}$ in Eq.4) is approximately 10 times greater than that of solids.

2.8.1.6 Sedimentation

Sedimentation rates in Aarhus Bay are found by interpretation of ^{210}Pb profiles. These interpretations are based on more recent and slightly more accurate mathematical modelling than used previously and, therefore, we have calculated a sedimentation rate
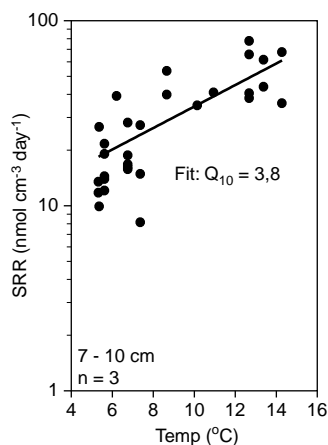

Figure 2.6. The Q_{10} value of 3.8 calculated for the primary reactions is based on the correlation between temperature and sulphate reduction rates in the depth interval 7-10 cm in Aarhus Bay. Note the logarithmic SRR scale. See text for further discussion of the figure.

48

approximately 2.5 times higher than that reported by the HAV90 studies in Aarhus Bay. In a modelling context sedimentation rate is a very important parameter, because permanent burial of solids in the seabed is directly proportional to this rate.

2.8.1.7 Irrigation

Irrigation is generally the dominant form of transport, for instance when it comes to removal of CO_2 from the seabed. Therefore, the irrigation parameter (α, see equation Eq.6) is initially assessed on the basis of profiles and production of CO_2. It should be noted, however, that sediment profiles of CO_2 were not determined in Aarhus Bay in the HAV90 programme. For use in the model it was therefore necessary to determine the irrigation parameter on the basis of a few CO_2 measurements made in 2000, which makes this determination somewhat uncertain.
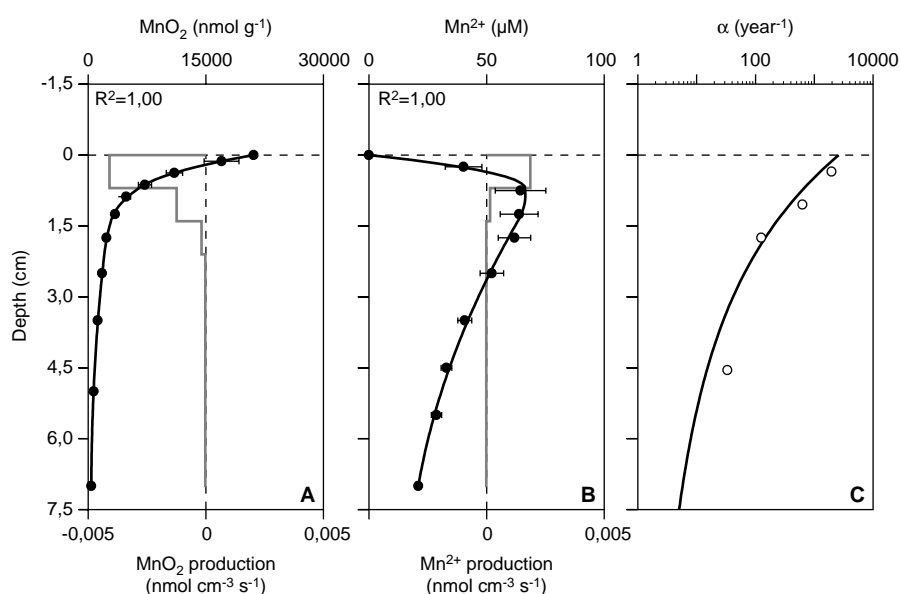
Figure 2.7. The irrigation parameter (α) as a function of depth based on concentration profiles of MnO_2, Mn^{2+} and CO_2 (Aarhus Bay). A: MnO_2 concentration and calculated MnO_2 consumption (negative rate). B: Mn^{2+} concentration and calculated Mn^{2+} production (positive rate) by reduction of MnO_2. C: Irrigation parameter (circles) calculated on the basis of consumption and production, respectively, of MnO_2 and Mn^{2+} and compared with calculations of CO_2 concentrations and production in the seabed (solid line). See text for discussion of preconditions for calculating the irrigation parameter.

Instead of using the irrigation parameter calculated for 2000 uncritically in the sediment flux model, we have verified the irrigation parameter by interpreting profiles of MnO_2 and Mn^{2+}, which were measured frequently during the HAV90 programme (1990-1991). In the model manganese can exist in the sediment in two different states; solid state (MnO_2) and dissolved state (Mn^{2+}). It is obvious, therefore, that production of one pool at a given depth must be balanced by a corresponding consumption of the other pool. The shape of the concentration profile of MnO_2 and Mn^{2+}, respectively, does in fact reflect production and consumption of the substances,

and because irrigation only influences the Mn^{2+} ion, any imbalance in this account can be used to quantify the significance of irrigation and hence the value of the irrigation parameter. Figure 2,7 shows the result of interpretations such as these and the irrigation parameter derived from them. The figure demonstrates a fair agreement between interpretation of Mn^{2+} and MnO_2 profiles and the somewhat uncertain calculation of the irrigation parameter based on concentration profiles of CO_2 from 2000.

2.8.1.8 Adsorption

The adsorption constants of Mn^{2+} and Fe^{2+} were determined on the basis of specific measurements made in Aarhus Bay. The constants for NH_4^+ and PO_4^{3-} were determined on the basis of mean values found in the literature, and are considerably lower than the corresponding constants for Mn^{2+} and Fe^{2+}.

2.8.1.9 The diffusive boundary layer

Sediment oxygen concentrations were measured using microelectrodes with a depth resolution of 100 μm. This makes it possible to determine the extent of the diffusive boundary layer, i.e. the width of the part of the oxygen profile exhibiting a linear decline in oxygen concentration. Microelectrode measurements show that the thickness of the diffusive boundary layer is approximately 0.03 cm.

2.8.1.10 Flux of manganese, iron and organic matter

As described previously, the external fluxes of MnO_2 and FeOOH to the sediment surface are equivalent to the amounts of manganese and iron, respectively, buried in the seabed and thus disappearing from the model. Sediment concentrations of both manganese and iron have been measured, and the sedimentation rate is known, and the fraction of the two compounds that is buried in the seabed is thus easy to calculate.

The ratio of the flux of undegraded organic matter ($F_{OM\,n}$) to total organic matter flux ($F_{OM\,total}$) is calculated from the concentration of organic matter at the bottom of the model (at a depth of 20 cm) and the sedimentation rate. Therefore, it is a prerequisite to the calculation that all degradable organic material has been degraded when this depth is reached. The ratio of the flux of readily degradable organic matter ($F_{OM\,r}$) to the total organic matter flux ($F_{OM\,total}$) was determined from literature values.

2.8.2 Input determined to some extent during the run-in phase of the model

A large group of model constants are determined to some extent in the run-in phase. Most often, we begin by estimating or guessing the value of a constant and letting the model carry out a calculation, after which the value is adjusted on the basis of comparison between calculated and measured values.

The many different constituent parts of the model are very closely linked – so closely that very few constants are determined one by one without affecting other model constants. In many cases a certain number of constants are therefore assigned their values in the same

50

optimisation procedure. A good example is the carbon cycle, the constants of which it is possible to determine before concentrating on the other cycles.

Up till now, it has been our experience that it is crucial to have a very detailed set of measured data available in the run-in phase of the model. Otherwise, the values of some constants will inevitably be assigned on an insufficient basis. It should be noted, however, that many constants are more or less universal and hence transferable from one type of sediment to another.

The many detailed measurements performed in the HAV90 programme cover the dynamics of the seabed during more than a year (January 1990-May 1991) and one of the goals of the model set-up is to be able to reproduce these dynamics by modelling. However, seasonal variations are too difficult to tackle in the run-in phase, and in many instances it is impossible to distinguish natural variations in the seabed from seasonal fluctuations. Therefore, the model constants were determined after the model had calculated data under stationary conditions and compared these data with mean values of data measured in the course of a year. We say that the model is in a stationary state. Here, stationary state refers to the fact that all the boundary conditions laid down in the model, such as bottom-water concentrations and organic matter fluxes, correspond to the mean values of one year's measurements. Likewise, all temperature-dependent sediment parameters, such as diffusivity, are determined using the mean sediment temperature, which is 9 $^{\circ}$C. For all substances, dissolved and solid alike, a concentration gradient of 0 was specified as the lower boundary condition. This boundary condition allows concentrations to vary freely between successive calculations at the bottom of the calculation zone. As the upper boundary condition a constant flux is specified for organic material. The boundary condition for all dissolved substances corresponds to the mean value of bottom-water concentrations measured in the course of a year.

C:N and C:P ratios. Initially, we estimated the C:N and C:P ratios of organic matter degradation on the basis of literature values. It is important to keep in mind that these ratios are not the total C:N and C:P ratios normally measured in sediments. After the model is partially run in, both ratios are adjusted so that the profiles of NH_4^+ and PO_4^{3+}, respectively, coincide with the measured profiles. As shown later, we have achieved a good agreement for both substances without letting the C:N and C:P ratios vary with depth.

The limiting concentrations e.g. $O_{2\,lim}$, $NO_{3\,lim}^-$, $MnO_{2\,lim}$ and $FeOOH_{lim}$ (see section 2.4.1) are initially estimated on the basis of literature values and experience with previous model set-ups. When the model is partially run in, concentrations are adjusted.

Rate constants. The majority of the rate constants are determined in two steps. First, preliminary values are found, after which final adjustment takes place. To that end, numerous comparisons are made between calculated and measured values, which are too extensive to

Degradation of OM$_s$ (nmol cm^{-3} s^{-1})

$K_{OMs}=$
9,0 10^{-9} s^{-1}
1,0 10^{-9} s^{-1}
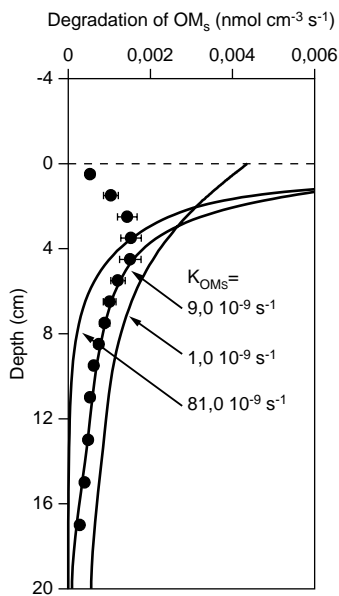81,0 10^{-9} s^{-1}

Depth (cm)

Figure 2.8. Calculation of the rate constant of the pool of slowly degradable organic matter, which below a certain depth is degraded exclusively by sulphate reduction. Calculated degradation rates of the slowly degradable pool are shown for three different rate constants (solid lines) together with measured sulphate reduction rates (black dots; Aarhus Bay). See text as well.

be presented here. We will therefore confine ourselves to giving a few examples.

The rate constant of the pool of slowly degradable organic matter is a very critical input parameter to the model and is determined on the basis of the average of one year's sulphate reduction profiles. Obviously, the pool of readily degradable organic matter is used up in the uppermost zone of the sediment, while "the slow pool" penetrates considerably further into the sediment before being degraded. This means that below a certain depth sulphate reduction originates exclusively in the degradation of slowly degradable organic matter. We exploit this fact in order to determine the rate constant of the slowly degradable organic matter pool. Figure 2.8 shows how the model has calculated the degradation rate of the slow pool as a function of depth at three different rate constants, 10^{-9} s^{-1}, 9×10^{-9} s^{-1} and 81×10^{-9} s^{-1}, respectively. The figure shows that the larger rate constant leads to too rapid degradation of the CH_2O_s pool, which as a result does not penetrate into the sediment far enough to support sulphate reduction. The reverse is the case for the smaller rate constant, whereas the rate constant of 9×10^{-9} s^{-1} gives a good agreement between calculated and measured sulphate reduction rates. Subsequently, the rate constant is adjusted slightly to its final value of 12×10^{-9} s^{-1}.

The rate constant of the pool of readily degradable organic matter is found in the same way, but uppermost in the sediment, where oxygen consumption is the factor determining the degradation rate of "the fast pool". The ratio between the rate constants of the "slow" and the "fast" pool in Aarhus Bay is approximately 800, which agrees well with ratios found in similar studies.

The remaining rate constants are found through similar reasoning or in the literature. The purpose of the model is to calculate concentration profiles of all dissolved and solid substances entering into the model. On the basis of these the model will be able to finally calculate oxygen and nutrient fluxes between seabed and bottom water and material transport within the seabed. Therefore, one of the most important purposes of running in the model has been to reproduce the measured concentration profiles. Initially, we have "only" calculated the profiles as yearly averages and compared them with averages of the profiles measured in the course of the "model year". The results of these calculations are shown in Figure 2.9 after determination of all constants and other model input. The figure clearly indicates an excellent agreement between modelled and measured concentration profiles of all substances shown.

The HAV90 programme did not focus only on concentration measurements in the seabed. Several degradation processes were measured as well; e.g. sulphate reduction rates. The model calculates sulphate reduction rates from concentration profiles of CH_2O_f and CH_2O_s (see Eq.15), temperature and the assigned constants. Figure 2,10 shows how well the model actually calculates sulphate reduction rates compared with annual averages of the measured rates. Here, too, the model reproduces the measured results satisfactorily.
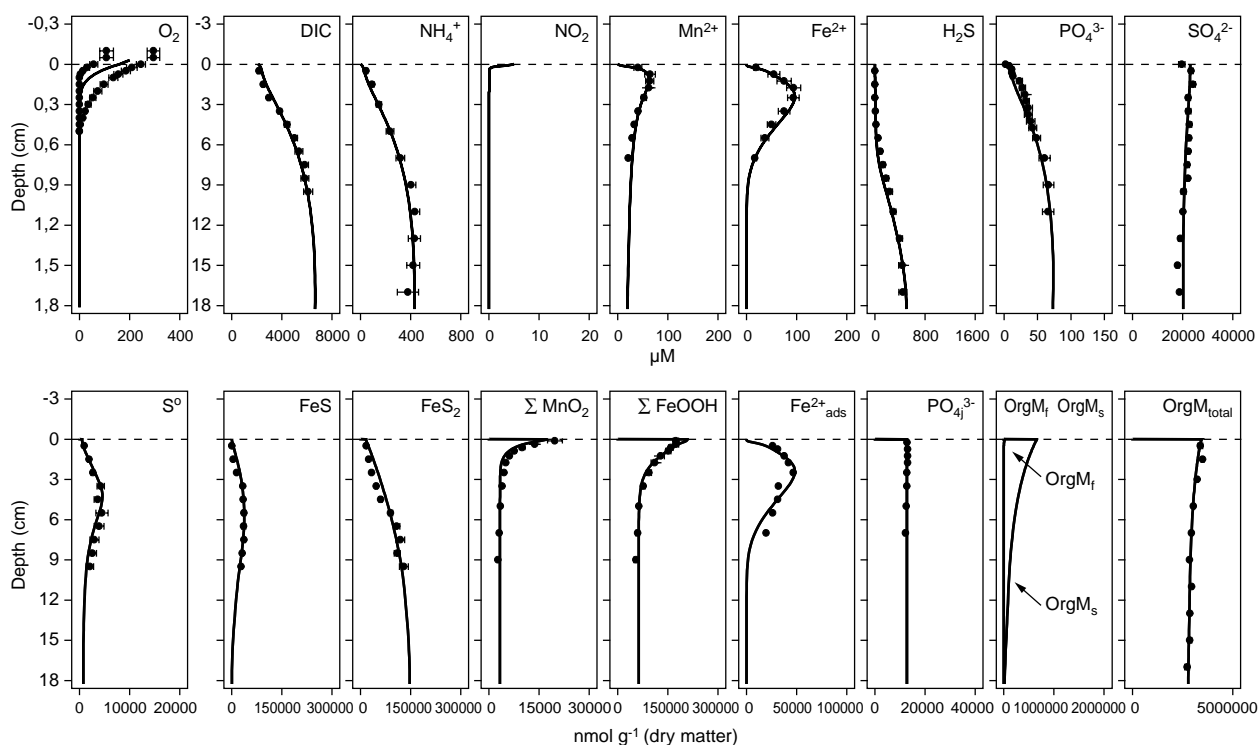
Figure 2.9. Concentration profiles of all chemical substances entering into the model, measured in Aarhus Bay during the HAV90 programme. Measured concentrations (black dots) are averaged over the HAV90 year and compared with the sediment flux model's stationary concentration profiles (solid lines). Oxygen concentrations vary markedly over the year and therefore the measured values are shown at both the largest and smallest oxygen penetration depths. Note the difference between the depth scale of oxygen (0-1.8 cm) and that of the other profiles (0-18 cm).

2.9 Dynamic calculation of the HAV90

The stationary model is able to convincingly reproduce all annual averages of the measured variables wherever comparison has been possible (Figures 2.9 and 2.10). Thus, the next step in the verification of the model is to examine its ability to predict the dynamic variation measured during the HAV90 year (1 Jan-31 Dec 1990).

Before we take the step of rendering the model dynamic, some small adjustments must be made to the stationary model. These adjustments affect boundary conditions and the temperature correction of diffusivity and process rates. The latter change is indicated in Table 2.2.

2.9.1 Boundary conditions in the dynamic model

As regards boundary conditions of solutes, bottom-water concentrations must be specified for every single day in 1990. Obviously, measurements have not been made this frequently, so we have calculated daily concentrations by linear interpolation. Actual measurements have typically been made at 1-4 week intervals, more frequently in spring and summer. All other substances have been assigned the same boundary conditions as in the stationary calculation, with the exception of organic matter. The variation in organic load to the sediment corresponds to primary production
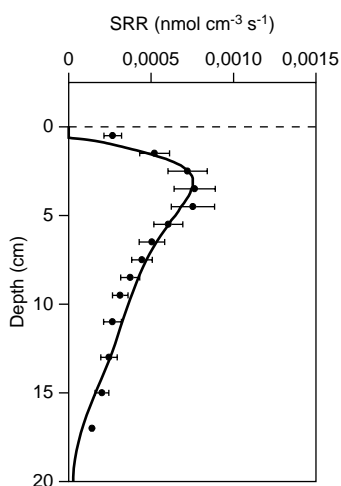

Figure 2.10. Modelled sulphate reduction rate (SRR; solid line) in the stationary sediment flux model compared with the annual average of measured rates (black dots; Aarhus Bay).

while its magnitude follows the production of CO_2 in the seabed, as discussed in the next section.

2.9.2   Organic load to the sediment

As mentioned previously the load of organic carbon to the seabed is an important parameter in the model. Organic material fuels the model, so to speak, as primary and secondary reactions all depend on the load of organic carbon and the N and P added to the sediment in the form of organic material.

When we wish to go over the calculation of scenarios in Aarhus Bay and need the organic load to the sediment as an input parameter we run into a problem, however, because the County of Aarhus does not measure organic load. Therefore, we have chosen to express the best estimate of the organic load to the sediment in terms of particulate pelagic primary production, which is routinely measured by the County of Aarhus.

By doing so we achieve
*   a "natural" seasonal variation in organic load to the sediment corresponding to the variation in primary production. In other words, the organic load to the sediment reacts to the production of organic matter in the water column
*   a year-to-year variation in organic load to the sediment, as primary production varies from year to year.

Based on knowledge of annual primary production we calculate the annual variation in organic load to the sediment. This is only partly true, of course, but the only way we can produce a reasonable estimate of the organic load to the sediment is by linking it to pelagic primary production. Our calculation of the sedimentation of organic carbon is performed on the basis of the following considerations (Table 2.3).

In the HAV90 year we can indirectly calculate the organic load to the sediment because it corresponds to the CO_2 flux from the sediment, which was calculated at 9.76 mol C m^{-2} $year^{-1}$. From the sediment concentration profile of organic carbon and the sedimentation rate we calculate that 0.84 mol C m^{-2} $year^{-1}$ disappears through the bottom of the model at a depth of 20 cm. This pool corresponds to the undegradable portion of the organic load to the sediment. Thus, we calculate that in the HAV90 year the total organic load to the sediment was (9.76 + 0.84 =) 10.60 mol C m^{-2} $year^{-1}$.

In the HAV90 year <u>total</u> primary production was 23.89 mol C m^{-2} $year^{-1}$ and the intrinsic respiration of the water column was 22.05 mol O_2 m^{-2} $year^{-1}$, corresponding to 16.54 mol C-eq. m^{-2} $year^{-1}$ at a respiratory coefficient of 0.75, i.e. the efficiency with which bacteria exploit their oxygen uptake in order to degrade organic material. In other words, in the HAV90 year (23.89–16.54)=7.35 mol C-eq. m^{-2} $year^{-1}$ reaches the seabed. Since the annual organic load to the sediment should be 10.60 mol C m^{-2} $year^{-1}$ there is a deficit of (10.60–7.35)=3.25 mol C m^{-2} $year^{-1}$. In accordance with the HAV90 programme an amount of organic material corresponding to the

calculated deficit should be transported from land and from adjacent water bodies (the Kattegat) to Aarhus Bay (see Table 2.3). Thus, the total organic load to the sediment of Aarhus Bay corresponds to $(10.60/23.89) \times 100 = 44\%$ of total primary production.

As mentioned previously, the County of Aarhus measures <u>particulate</u> primary production, which was 16.90 mol C-eq. m^{-2} year^{-1} in the period 1 May 1990-30 April 1991, i.e. $(16.90/23.89) \times 100 = 71\%$ of total primary production. This means that an organic input corresponding to $(10.60/16.90) \times 100 = 63\%$ of particulate primary production is added to the sediment.

Table 2.3. Primary production and organic C load to and consumption in the seabed.

Primary production (1.5.90-30.4.91)		
Total primary production[1,3]	23.89 mol C m^{-2} year^{-1}	
Particulate primary production[2,3]	16.90 mol C m^{-2} year^{-1}	
	HAV90 mol C m^{-2} year^{-1}	Contribution of particulate primary production
Primary production[1]	23.89	1.41
Intrinsic water-column respiration[4] 22.05 mol O_2 m^{-2} år^{-1}	16.54[4]	0.98
Remainder, i.e. sedimentation from above water column	7.35	0.43
Organic material from other sources	3.25	0.19
Total organic load to the seabed	10.60	0.63
Undegraded organic material	0.84	0.05
Degraded organic material	9.76	0.58

1) Measured in the HAV90 programme.
2) Measured routinely by the County of Aarhus in the monitoring of Aarhus Bay.
3) Particulate primary production/total primary production = 0.8, determined from mean values from 4 years in which both measurements were performed: 0.84±0,09 (see text).
4) Calculated value at a respiratory coefficient of 0.75.

2.9.3   The sediment flux model simulates the HAV90 year

The starting point of the model's simulation of the HAV90 year is arbitrarily set to year 0. At this point the concentrations of all substances in all sediment layers are 0. On 1 January in the year 0 sedimentation of organic material and addition of FeOOH and MnO_2 to the sediment begin. At the same time, O_2, NO_3^-, NH_4^+, PO_4^{3-} and SO_4^{2-} begin to move downwards through the sediment layers by diffusion, bioturbation and bioirrigation. As substances gradually "arrive" in the various sediment layers, degradation sets in – if conditions allow, that is. Gradually, the concentration profiles of the different substances begin to take shape. One year later (31 December in the year 0) concentration profiles of most substances can be seen in the uppermost layers of the model, but these profiles are far from corresponding to the concentrations measured in the HAV90

programme. Therefore, the model goes through the HAV90 year calculations once again. In this way, the HAV90 year is run again and again until a quasi-stationary equilibrium is achieved in the sediment, meaning that concentration profiles may vary over a year, but on one specific date, profiles, fluxes etc. are the same from year to year.

As mentioned previously, the model consists of layers extending to a depth of 20 cm. The sedimentation rate is calculated at 0.064 cm year^{-1}, meaning that on average (20/0.064)=310 years elapse from a sediment particle lands on the sediment surface till it reaches a depth of 20 cm and disappears from the model. Due to the influence of bioturbation on particles the model does not approach a stationary situation until at least 5 times that amount of time has passed, i.e. more than 1500 years (Figure 2.11).
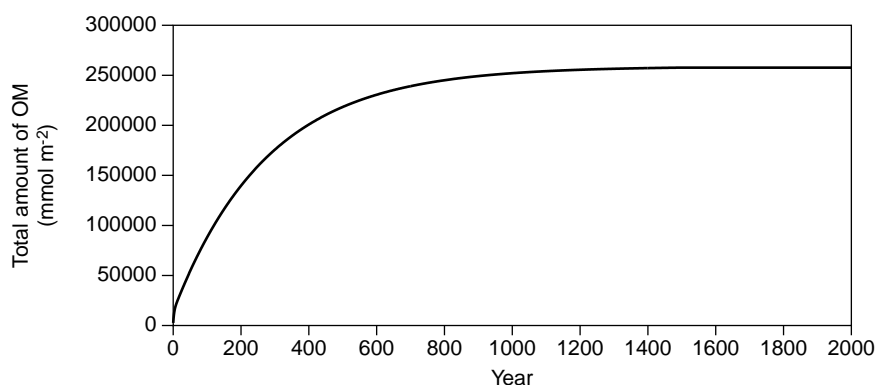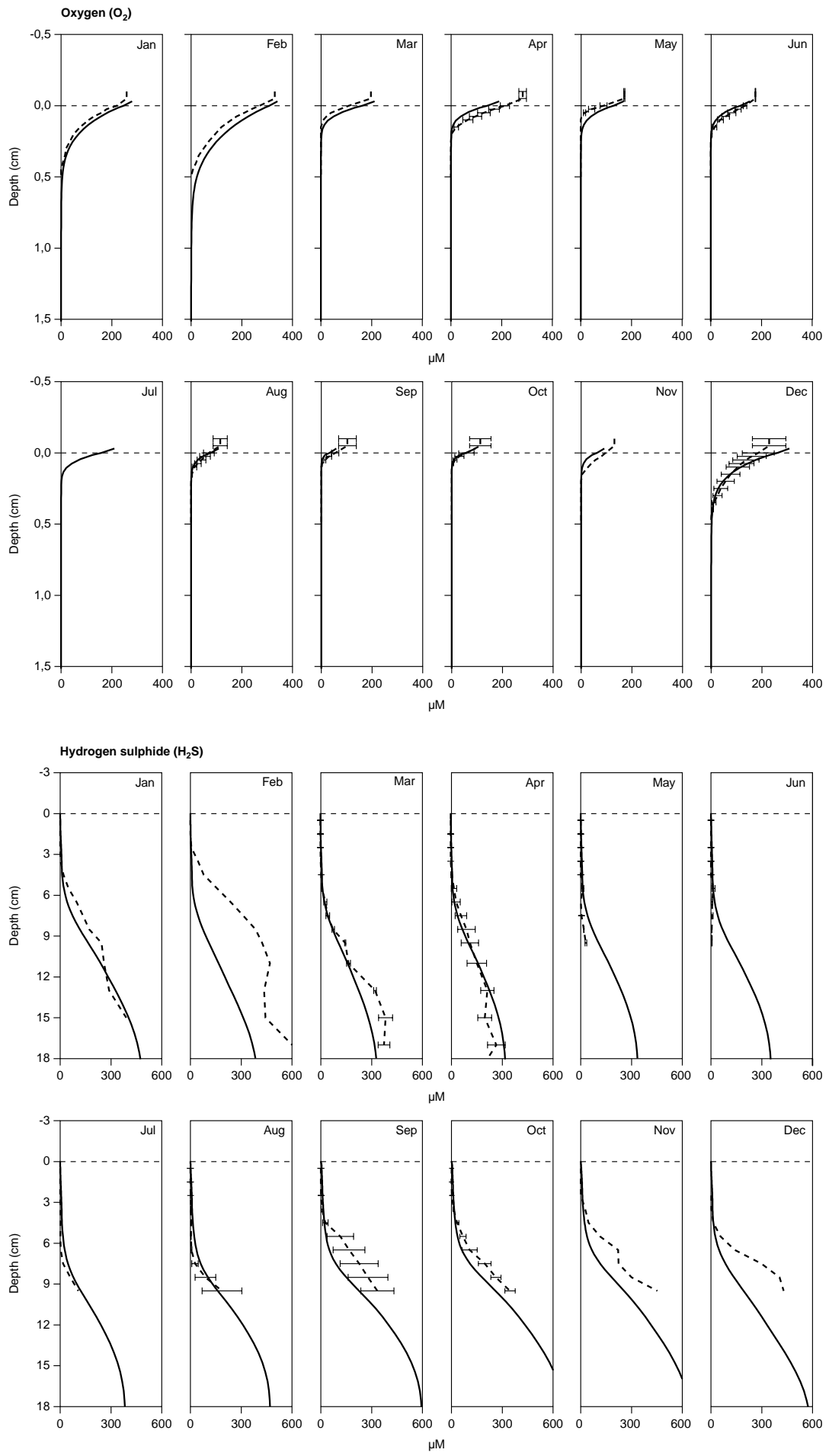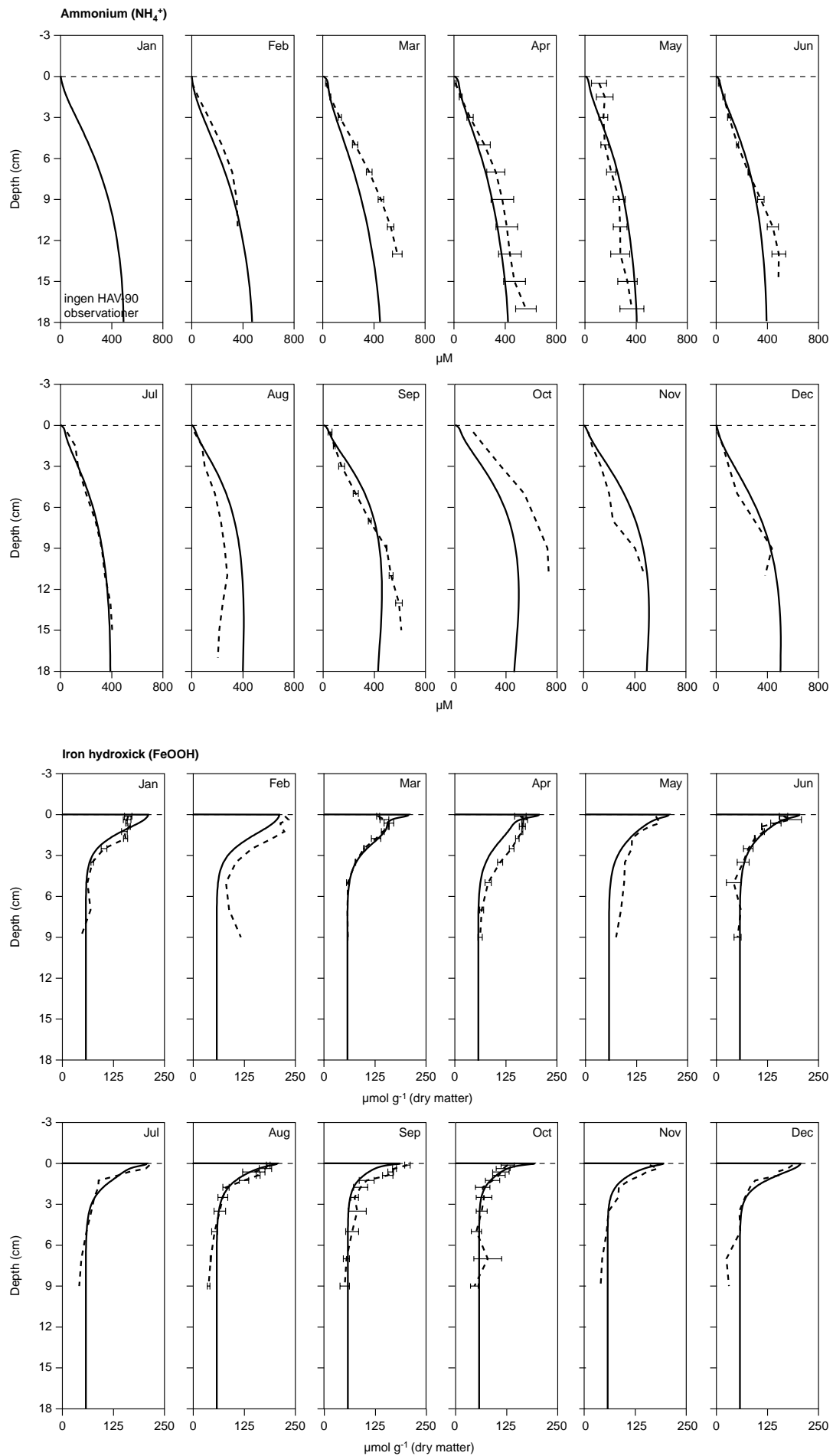

Figure 2.11. The total amount of organic material (0-20 cm) as a function of time (years), the sedimentation of organic matter starting at year 0.

Figure 2.12 demonstrates how well the concentration profiles of a number of substances modelled by the dynamic model simulate the HAV90 year in all 12 months of the year. The data underlying the concentration profiles in the figure represent model output extracted at noon on the 15th of each month and are shown together with mean values of observations from the HAV90 programme ±standard error, when 2 or more measurements were made in the month in question. The figure clearly indicates an excellent agreement between modelled and measured concentration profiles of all substances shown.
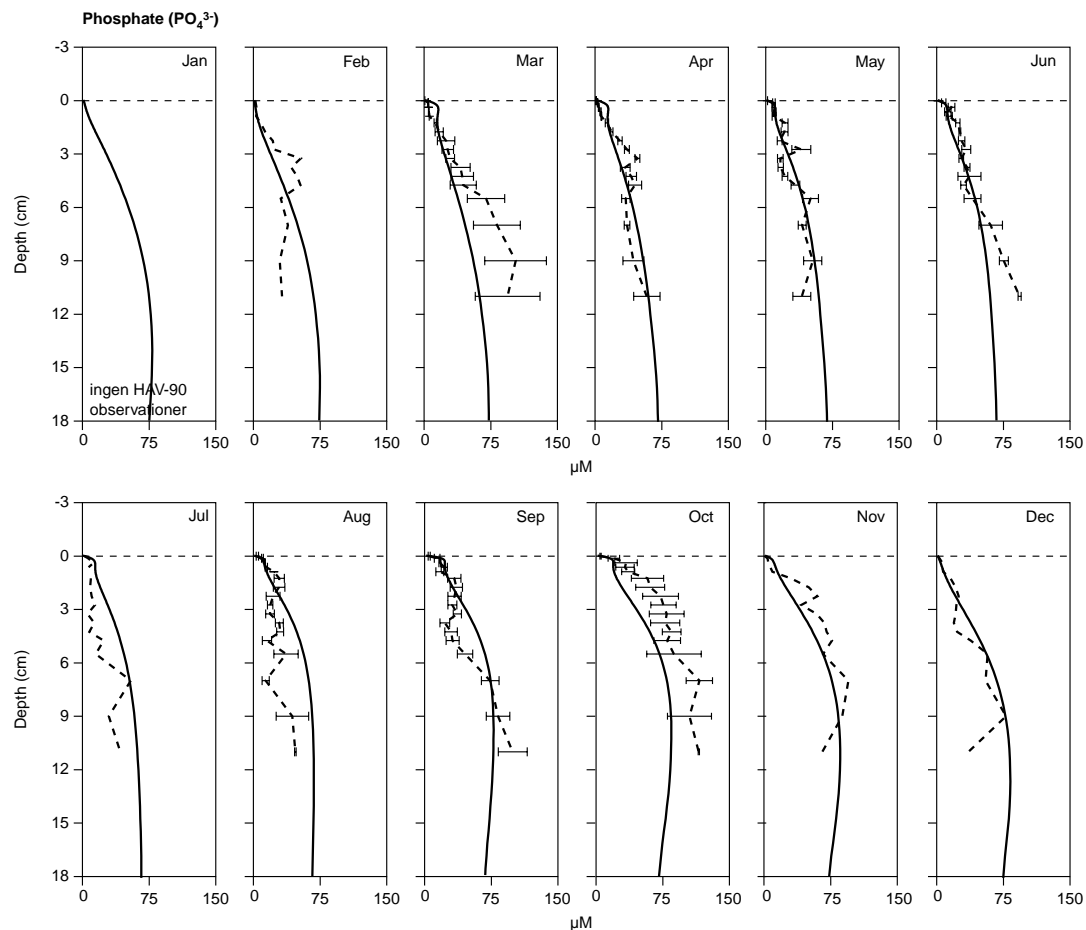
Oxygen (O₂)

Hydrogen sulphide (H₂S)

Ammonium (NH$_4^+$)

μM

μM

Iron hydroxick (FeOOH)

μmol g^{-1} (dry matter)

μmol g^{-1} (dry matter)

58

Phosphate (PO₄³⁻)

Figure 2.12. Concentration profiles of selected substances measured and modelled by the dynamic model in all 12 months of the year: oxygen (O₂), hydrogen sulphide (H₂S), ammonium (NH₄⁺), iron hydroxide (FeOOH) and phosphate (PO₄³⁻) in Aarhus Bay. The modelled profiles (solid lines) are model output from noon on the 15th on the month in question. Measured concentrations (broken lines) represent monthly observations or monthly mean values ±standard error, if two or more measurements were made that month. Note the difference between the depth scale of oxygen (0-1,5 cm) and that of the other profiles (0-18 cm).

Just like the stationary modelling, the dynamic modelling of process and flux rates in the HAV90 year can be compared with true measurements. This comparison shows that the dynamic model is quite capable of simulating the HAV90 year. We will verify this by giving a few examples.

The model calculates both the diffusive and the total O₂ flux (Figure 2.13). In the HAV90 programme oxygen uptake was measured in intact sediment cores each representing a 20-cm² area of the seabed. This is an important point in the comparison of modelled and measured oxygen uptake. Ideally, measured O₂ uptake should correspond to modelled total uptake, but this is not the case. The similarity to the diffusive O₂ flux is considerably greater to the point of being almost identical. It is very likely, therefore, that both bioirrigation and bioturbation are limited or even cease altogether when the 20 cm² of seabed is confined to a Plexiglas tube. Under these circumstances the O₂ flux will come to be dominated entirely by diffusive oxygen uptake, and, consequently, we are quite pleased with our modelling of the O₂ flux.
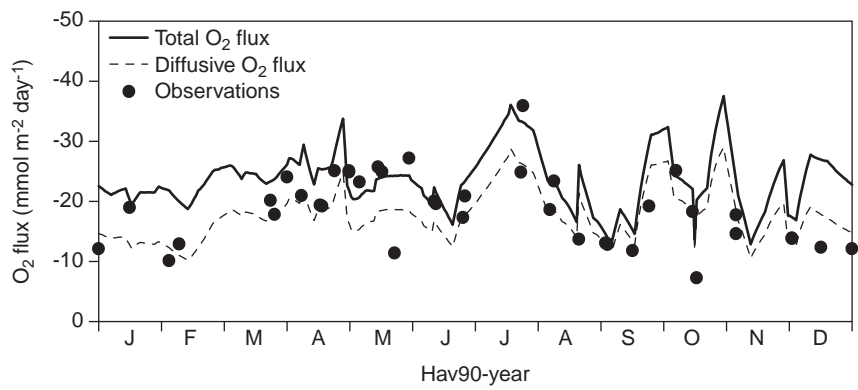
Figure 2.13. Modelled total and diffusive oxygen flux in the HAV90 year compared with values measured in Aarhus Bay. Note the near to identical nature of measured and diffusive oxygen uptake. This is due to the bioactivity being strongly reduced in laboratory set-ups causing measured uptake to be smaller that the modelled total (or *in situ*) oxygen uptake.

Like O_2 flux, the sulphate reduction rate is measured in intact cores, but sulphate reduction is influenced by neither bioturbation nor bioirrigation in the short term, i.e. from collection of the cores to measurement of the rates. However, the measured sulphate reduction rate exhibits a great deal of "noise", especially in summer and autumn, giving the rate a "jagged" appearance. This may be due to inhomogeneity in the seabed, and differences in the sediment from one sampling to another. Remember that one measurement covers only 20 cm^2 of the seabed, which explains the scatter displayed by the measured sulphate reduction rates. Therefore, we believe that the model is capable of calculating an adequate mean value of the sulphate reduction rate in Aarhus Bay.
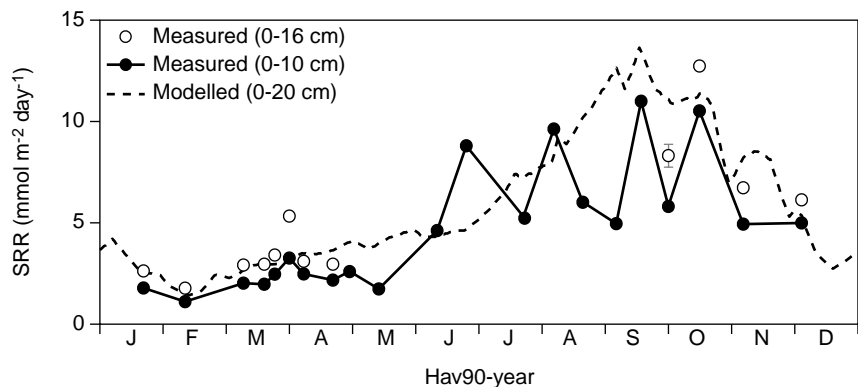

Figure 2.14. Modelled and measured sulphate reduction rates (SRR) in Aarhus Bay during the HAV90 year.

2.9.4 Evaluation of the sediment flux models simulation of the HAV90 year

Generally, the agreement is exceptionally good between observations made in the HAV90 year and the concentration profiles calculated by the model (Figure 2.12).

There are, of course, months in which the modelled concentration profile diverges from HAV90 measurements, but this does not

necessarily mean that the profile calculated by the model that particular month is wrong. The reason may just as well be that the HAV90 measurement made that month deviates from the "norm". In the real world, the sediment of Aarhus Bay is heterogeneous and not the homogeneous mass applied in the model. A certain amount of scatter in the analytical results from the HAV90 programme is to be expected and a 100% agreement between modelled and actual concentration profiles, or process rates for that matter, is not possible, as discussed in connection with sulphate reduction rates. It should be noted, however, that there is no tendency towards the model over- or underestimating modelled data compared with measured values.

We therefore conclude that
- the sediment flux model simulates concentration profiles in the sediment of Aarhus Bay realistically.
- the sediment flux model responds dynamically to addition of organic matter to the sediment in such a way that in a given season concentration profiles adjust as expected. Therefore, the model is able to also calculate nutrient fluxes between seabed and bottom water realistically.
- the sediment flux model is well-suited for simulating the response of the seabed to changes in organic loads, bottom-water oxygen concentrations, nutrient concentrations etc. All it takes is to alter the input parameters to the model in accordance with the scenario laid out.

[Blank page]

Background information and where to read more

Berg, P., Rysgaard, S. & Thamdrup, B. (in press) Dynamic modeling of early diagenesis and nutrient cycling: A case study in an Arctic marine sediment. American Journal of Science

Christensen, P.B. (Ed.) (1998) The Danish marine environment: Has action improved its state? Conclusions and perspectives of the Marine Research Programme HAV90. Havforskning fra Miljøstyrelsen, Vol. 62, Danish Environmental Protection Agency, Copenhagen.

Glud, R.N., Gundersen, J.K., Røy, H. & Jørgensen, BB. (2003) Seasonal dynamics of benthic O_2 uptake in a semienclosed bay: Importance of diffusion and faunal activity. Limnology and Oceanography 48, 1265-1276.

Glud, R.N., Gundersen, J.K., Jørgensen, B.B., Revsbech, N.P. & Hüttel, M. (1994) Calibration and performance of the stirred chamber from the benthic flux-chamber lander ELINOR. Deep-Sea Research 42, 1029-1042.

Gundersen, J.K. & Jørgensen, B.B. (1990) Microstructure of diffusive boundary layer and the oxygen uptake of the sea floor. Nature 345,604-607.

Jensen, H.S., Mortensen, P.B., Andersen, F.Ø., Rasmussen, E. & Jensen, A. (1995) Phosphorous cycling in a coastal marine sediment, Aarhus Bay, Denmark. Limnology and Oceanography 40, 908-917.

Jensen, H.S. & Thamdrup, B. (1993) Iron-bound phosphorous in marine sediments as measured by bicarbonate.dithionite extraction. Hydrobiologia 253, 47-59.

Jensen, M.H., Andersen, T.K. & Sørensen, J. (1988) Denitrification in coastal bay sediment – regional and seasonal variation in Aarhus Bight, Denmark. Marine Ecology Progress Series 48, 155-162.

Jensen, M.H., Lomstein, E. & Sørensen, J. (1990) Benthic NH_4^+ and NO_3^- flux following sedimentation of a spring phytoplankton bloom in Aarhus Bight, Denmark. Marine Ecology Progress Series 61, 87-96

Jørgensen, B.B. (1995) Case study: Aarhus Bay, Chap. 7. In B.B. Jørgensen & K. Richardson (Eds.) Eutrophication in coastal marine ecosystem, American Geophysical Union

Kruse, B. (1993) Measurement of plankton O_2 respiration in gas-tight plastic bags. Marine Ecology Progress Series 94, 155-163

Moeslund, L., Thamdrup, B. & Jørgensen, B.B. (1994) Sulfur and iron cycling in a coastal sediment – radiotracer studies and seasonal dynamics. Biogeochemistry 27, 129-152.

Nielsen, L.P. & Glud, R.N. (1996) Denitrification in a coastal sediment measured in situ by the nitrogen pairing technique applied to a benthic flux chamber. Marine Ecology Progress Series 137, 181-186.

Pejrup, M., Valeur, J. & Jensen, A. (1995) Vertical fluxes of particulate matter in Aarhus Bight, Denmark. Continental Shelf Research 16, 1047-1064.

Rasmussen, H. & Jørgensen, B.B. (1992) Microelectrode studies of seasonal oxygen uptake in a coastal sediment: role of molecular diffusion. Marine Ecology Progress Series 81, 289-303.

Thamdrup, B., Fossing, H. & Jørgensen, B.B. (1994) Manganese, iron and sulfur cycling in a coastal marine sediment. Geochemica et Cosmochemica Acta 58, 5115-5129.

Thamdrup, B., Glud, R.N. & Hansen, J.W.(1994) Manganese oxidation and in situ manganese fluxes from a coastal sediment. Geochemica et Cosmochemica Acta 58, 2563-2570

Thamdrup B., Hansen, J.W. & Jørgensen, B.B. (1998) Temperature dependence of aerobic respiration in a coastal sediment. FEMS Microbiology Ecology 25, 189-200.

van Capellen, P. & Wang, Y. (1996) Cycling of iron and manganese in surface sediments: A general theory for the coupled transport and reaction of carbon, oxygen, nitrogen, sulfur, iron and manganese. American Journal of Science 296, 197-243.

Reports (in Danish) with observations and data used for the oxygen and nutrient flux model set-up (*in italics* English translation of Danish title)

Christiansen, C., Lund-Hansen, L.C. & Skyum, P. (1994) Hydrografi og stoftransport i Århus Bugt *(Hydrography and material transport in Aarhus Bay)*. Havforskning fra Miljøstyrelsen, Vol. 39, Danish Environmental Protection Agency, Copenhagen.

Floderus, S. (1992) Sedimentation og resuspension i Århus Bugt *(Sedimentation and resuspension in Aarhus Bay)*. Havforskning fra Miljøstyrelsen, Vol. 18, Danish Environmental Protection Agency, Copenhagen.

Fossing, H., Thamdrup, B. & Jørgensen, B.B. (1992) Havbundens svovl-, jern- og mangankredsløb i Århus Bugt *(Sulfur, iron, and manganese cycling in the sea floor of Aarhus Bay)*. Havforskning fra Miljøstyrelsen, Vol. 15, Danish Environmental Protection Agency, Copenhagen.

Hansen, J.W., Thamdrup, B., Fossing, H. & Jørgensen, B.B. (1994) Redoxbalancen og mineraliseringens temperaturafhængighed i Århus Bugt *(Redox balance and temperature regulation of mineralization in Aarhus Bay).* Havforskning fra Miljøstyrelsen, Vol. 36, Danish Environmental Protection Agency, Copenhagen.

Gundersen, J.K., Glud, R.N. & Jørgensen, B.B. (1995) Havbundens iltomsætning *(Oxygen uptake of the sea floor in Aarhus Bay).* Havforskning fra Miljøstyrelsen, Vol. 57, Danish Environmental Protection Agency, Copenhagen.

Jørgensen, B.B. (Ed.) (1995) Stoftransport og stofomsætning i Århus Bugt *(Material transport and mineralization in Aarhus Bay).* Havforskning fra Miljøstyrelsen, Vol. 59, Danish Environmental Protection Agency, Copenhagen.

Lomstein, B.Aa & Blackburn, T.H. (1992) Havbundens kvælstofomsætning i Århus Bugt *(Nitrogen cycling in the sea floor of Aarhus Bay).* Havforskning fra Miljøstyrelsen, Vol. 16, Danish Environmental Protection Agency, Copenhagen.

Mortensen, P.B., Jensen, H.S., Rasmussen, E.K. & Andersen, F.Ø. (1992) Fosforomsætning i sedimentet i Århus Bugt *(Phosphorous cycling in the sea floor of Aarhus Bay).* Havforskning fra Miljøstyrelsen, Vol. 17, Danish Environmental Protection Agency, Copenhagen.

Nielsen, J., Lynggaard-Jensen, A., Hansen, H.P. & Simonsen, C. (1993) Dynamik og kompleksitet i Århus Bugt *(Dynamics and complexity in Aarhus Bay).* Havforskning fra Miljøstyrelsen, Vol. 23, Danish Environmental Protection Agency, Copenhagen.

Valeur, J.R., Pejrup, M. & Jensen, A. (1992) Partikulære nærings-stoffluxe i Vejle Fjord og Århus Bugt *(Particulate nutrient fluxes in Vejle Fjord and Aarhus Bay).* Havforskning fra Miljøstyrelsen, Vol. 14, Danish Environmental Protection Agency, Copenhagen.

National Environmental Research Institute

The National Environmental Research Institute, NERI, is a research institute of the Ministry of the Environment.
In Danish, NERI is called Danmarks Miljøundersøgelser (DMU).
NERI's tasks are primarily to conduct research, collect data, and give advice on problems related to the environment and nature.

Faglige rapporter fra DMU/NERI Technical Reports

2003

Nr. 436: Naturplanlægning - et system til tilstandsvurdering i naturområder. Af Skov, F., Buttenschøn, R. & Clemmensen, K.B. 101 s. (elektronisk)

Nr. 437: Naturen i hverdagslivsperspektiv. En kvalitativ interviewundersøgelse af forskellige danskeres forhold til naturen. Af Læssøe, J. & Iversen, T.L. 106 s. (elektronisk)

Nr. 438: Havternen i Grønland. Status og undersøgelser. Af Egevang, C. & Boertmann, D. 69 s. (elektronisk)

Nr. 439: Anvendelse af genmodificerede planter. Velfærdsøkonomisk vurdering og etiske aspekter. Af Møller, F. 57 s. (elektronisk)

Nr. 440: Thermal Animal Detection System (TADS). Development of a Method for Estimating Collision Frequency of Migrating Birds at Offshore Wind Turbines. By Desholm, M. 25 pp. (electronic)

Nr. 441: Næringsstofbalancer på udvalgte bedrifter i Landovervågningen. Af Hansen, T.V. & Grant, R. 26s. (elektronisk)

Nr. 442: Emissionsfaktorer og emissionsopgørelse for decentral kraftvarme. Eltra PSO projekt 3141. Kortlægning af emissioner fra decentrale kraftvarmeværker. Delrapport 6. Af Nielsen, M. & Illerup, J.B. 113 s. (elektronisk)

Nr. 443: Miljøøkonomisk analyse af skovrejsning og braklægning som strategier til drikkevandsbeskyttelse. Af Schou, J.S. 43 s. (elektronisk)

Nr. 444: Tungmetaller i tang og musling ved Ivittuut 2001. Af Johansen, P. & Asmund, G. 32 s. (elektronisk)

Nr. 445: Modeller til beskrivelse af iltsvind. Analyse af data fra 2002. Af Carstensen, J. & Erichsen, A.C. 60 s. (elektronisk)

Nr. 447: Modelanalyser af mobilitet og miljø. Slutrapport fra TRANS og AMOR II. Af Christensen, L. & Gudmundsson, H. 114 s. (elektronisk)

Nr. 448: Newcastle Disease i vilde fugle. En gennemgang af litteraturen med henblik på at udpege mulige smittekilder for dansk fjerkræ. Af Therkildsen, O.R. 61 s. (elektronisk)

Nr. 449: Marin recipientundersøgelse ved Thule Air Base 2002. Af Glahder, C.M. et al. 143 s. (elektronisk)

Nr. 450: Air Quality Monitoring Programme. Annual Summary for 2002. By Kemp, K. & Palmgren, F. 36 pp. (electronic)

Nr. 451: Effekter på havbunden ved passage af højhastighedsfærger. Af Dahl, K. & Kofoed-Hansen, H. 33 s. (elektronisk)

Nr. 452: Vingeindsamling fra jagtsæsonen 2002/03 i Danmark. Wing Survey from the 2002/03 Hunting Season in Denmark. Af Clausager, I. 66 s.

Nr. 453: Tålegrænser for kvælstof for Idom Hede, Ringkøbing Amt. Af Nielsen, K.E. & Bak, J.L. 48 s. (elektronisk)

Nr. 454: Naturintegration i Vandmiljøplan III. Beskrivelse af tiltag der, ud over at mindske tilførsel af næringssalte fra landbrugsdrift til vandområder, også på anden vis kan øge akvatiske og terrestriske naturværdier. Af Andersen, J.M. et al. 67 s. (elektronisk)

Nr. 455: Kvantificering af næringsstoffers transport fra kilde til recipient samt effekt i vandmiljøet. Modeltyper og deres anvendelse illustreret ved eksempler. Nielsen, K. et al. 114 s. (elektronisk)

Nr. 456: Opgørelse af skadevirkninger på bundfaunaen efter iltsvindet i 2002 i de indre danske farvande. Af Hansen, J.L.S. & Josefson, A.B. 32 s. (elektronisk)

Nr. 457: Kriterier for gunstig bevaringsstatus. Naturtyper og arter omfattet af EF-habitatdirektivet & fugle omfattet af EF-fuglebeskyttelsesdirektivet. Af Søgaard, B. et al. 2. udg. 460 s. (elektronisk)

Nr. 458: Udviklingen i Vest Stadil Fjord 2001-2002. Af Søndergaard, M. et al. 25 s. (elektronisk)

Nr. 459: Miljøøkonomiske beregningspriser. Forprojekt. Af Andersen, M.S. & Strange, N. 88 s. (elektronisk)

Nr. 460: Aerosols in Danish Air (AIDA). Mid-term report 2000-2002. By Palmgren, F. et al. 92 pp. (electronic)

Nr. 461: Control of Pesticides 2002. Chemical Substances and Chemical Preparations. By Krongaard, T., Petersen, K. & Christoffersen, C. 30 pp. (electronic)

Nr. 462: Bevaringsstatus for fuglearter omfattet af EF-fuglebeskyttelsesdirektivet. Af Pihl, S. et al. 130 s. (elektronisk)

Nr. 463: Screening for effekter af miljøfarlige stoffer på algesamfund omkring havneanlæg. Af Dahl, K. & Dahllöff, I. 37 s. (elektronisk)

Nr. 464: Dioxin i bioaske. Dioxinmåleprogram 2001-2003. Viden om kilder og emissioner. Af Hansen, A.B. et al. 40 s. (elektronisk)

Nr. 465: Miljøundersøgelser ved Maarmorilik 2002. Af Johansen, P., Riget, F. & Asmund, G. 62 s. (elektronisk)

Nr. 466: Atmosfærisk deposition 2002. NOVA 2003. Af Ellermann, T. et al. 88 s. (elektronisk)

Nr. 467: Marine områder 2002 - Miljøtilstand og udvikling. NOVA 2003. Af Rasmussen, M.B. et al. 103 s. (elektronisk)

Nr. 468: Landovervågningsoplande 2002. NOVA 2003. Af Grant, R. et al. 131 s. (elektronisk)

Nr. 469: Søer 2002. NOVA 2003. Af Jensen, J.P. et al. 63 s. (elektronisk)

Nr. 470: Vandløb 2002. NOVA 2003. Af Bøgestrand, J. (red.) 76 s. (elektronisk)

Nr. 471: Vandmiljø 2003. Tilstand og udvikling - faglig sammenfatning. Af Andersen, J.M. et al. 157 s., 100,00 kr.

Nr. 472: Overvågning af Vandmiljøplan II - Vådområder 2003. Af Hoffmann, C.C. et al. 83 s. (elektronisk)

Nr. 473: Korrektion for manglende indberetninger til vildtudbyttestatistikken. Af Asferg, T. & Lindhard, B.J. 28 s. (elektronisk)

Most of the organic matter found in the sea is degraded in the
seabed. A number of different bacteria are responsible for organic
matter degradation. Through their metabolic processes bacteria
form inorganic nitrogen and phosphorus compounds that are thus
made available for new production. They also produce a number of
waste products, such as hydrogen sulphide, that have a great
impact on the marine environment. After many years of research,
our knowledge of the processes going on in the seabed is
substantial. This knowledge forms the basis of a new mathematical
model linking the complex material cycles taking place in the
seabed and describing the exchange of oxygen and nutrients
between seabed and seawater. The construction of the model is
described in this report. This report was prepared as a contribution
towards developing NERI's expertise within the field of
mathematical modelling.